Geochimica et Cosmochimica Acta Vol. 57, pp. 3677–3704

0016-7037/93/$6.00 + .00

Isotopic and trace-element constraints on mantle and crustal contributions to Siberian continental flood basalts, Noril'sk area, Siberia

JOSEPH L. WOODEN,[1] GERALD K. CZAMANSKE,[1] VALERI A. FEDORENKO,[2] NICHOLAS T. ARNDT,[3] CATHERINE CHAUVEL,[3] ROBIN M. BOUSE,[1] BI-SHIA W. KING,[1] ROY J. KNIGHT,[4] and DAVID F. SIEMS[4]

[1]US Geological Survey, 345 Middlefield Rd., Menlo Park, CA 94025, USA
[2]Central Research Institute of Geological Prospecting for Base and Precious Metals, Varshavskoye Sh. 129B, Moscow 113545, Russia
[3]Géosciences Rennes, Université de Rennes 1, 35042 Rennes cedex, France
[4]US Geological Survey, Denver Federal Center, Denver, CO 80225, USA

(*Received July 22, 1992; accepted in revised form May 6, 1993*)

Abstract—We present a tightly controlled and comprehensive set of analytical data for the 250-Ma Siberian flood-basalt province. Consideration of major- and trace-element compositions, along with strontium, lead, and neodymium isotopic compositions, strongly supports earlier Russian subdivision of this magmatism into three magmatic cycles, giving rise to three assemblages of eleven basalt suites in the ascending order Ivakinsky-Gudchikhinsky, Khakanchansky-Nadezhdinsky, and Morongovsky-Samoedsky. Geochemical and isotopic discontinuities of varying magnitude characterize most of the boundaries between the eleven recognized basalt suites in the Noril'sk area.

Although we conclude that the dominant volume of erupted magma originated from an asthenospheric mantle plume, none of the lavas is interpreted to directly represent asthenospheric melts, which would have been far more magnesian. On the basis of thermal considerations, we consider it unlikely that vast volumes of basaltic melt were produced directly from the continental lithospheric mantle beneath the Siberian craton. Moreover, there is little evidence from mantle xenoliths that the geochemical signatures of such melts would correspond to those of the Siberian flood basalts. Studies of melt migration lead us to conclude that transport of asthenospheric melt through the lithospheric mantle would be rapid, by fracture propagation. Lavas from the Gudchikhinsky suite have negligible Ta-Nb anomalies and positive ϵ_{Nd} values, and their parental magmas presumably interacted little with the continental lithospheric mantle or crust. All other lavas have negative Ta-Nb anomalies and lower ϵ_{Nd} values that we attribute to interaction with continental crust.

The model that we have developed requires discrete contributions from the plume and complex processing of all erupted magmas in the continental crust. The earliest magmas represent small percentages of melt formed in equilibrium with garnet. Over time, the percentage of melting in the source region and the volume of magma produced increased, and garnet was no longer stable in the plume source. All of the plume-derived melts initially contained more than 20 wt% MgO and became less Mg rich by fractionation of olivine as they traversed the lithospheric mantle. We conclude, however, that the most significant control on the geochemical and isotopic compositions of all the erupted lavas was processing of mantle-derived magma in crustal reservoirs during periodic replenishment, periodic tapping, continuous crystal fractionation, and wallrock assimilation. Rapid eruption of an extremely large volume of processed magma that varied little in chemical and isotopic composition produced the sequence of relatively monotonous tholeiitic basalts that constitute the 2,300-m-thick third assemblage of the Siberian flood-basalt province near Noril'sk.

INTRODUCTION

THE OPPORTUNITY TO STUDY the Siberian flood-basalt province (SFBP) arose in 1990 through a joint memorandum of understanding between the USGS and the Ministry of Geology of the former USSR for study of the famed Noril'sk-Talnakh mining district of Siberian Russia (Fig. 1). These continental flood basalts (CFBs) not only are of extraordinary interest in their own right but also are related to the evolution of the magmatic ore deposits of Noril'sk-Talnakh, which constitute one of the outstanding mineralized districts in the world. These ore deposits are unique in their association with a flood basalt province; in the inordinate amount of magmatic sulfide ore found in association with mafic-ultramafic intrusions that are 15–18 km long, 1–3 km wide, and less than 350 m thick; and in the exceptionally high contents of Cu, Ni, and platinum-group elements (PGEs) in these ores (CZAMANSKE et al., 1992b; NALDRETT et al., 1992).

Because our investigation of the petrology, chemistry, and origin of the SFBP was directly motivated by a desire to understand the temporal and geochemical relations between this basaltic volcanism and the economically important ore-bearing intrusions—an effort that could lead to discovery of similar deposits associated with flood-basalt provinces elsewhere—our focus here is on characterization of the basaltic system in terms of its evolution and endmembers. The processes that modified the source magmas are of interest insofar as they may also be responsible for the variety of magmas recognized as having formed the ore-bearing intrusions and, in addition, the concentrations of sulfide melt associated with the intrusions. We are less concerned herein, however, with the challenge of addressing the much broader problems relevant to the origin of CFBs (e.g., CARLSON, 1991). Nonetheless, largely because it appears to represent the most viable means of generating large volumes of basaltic magma in a

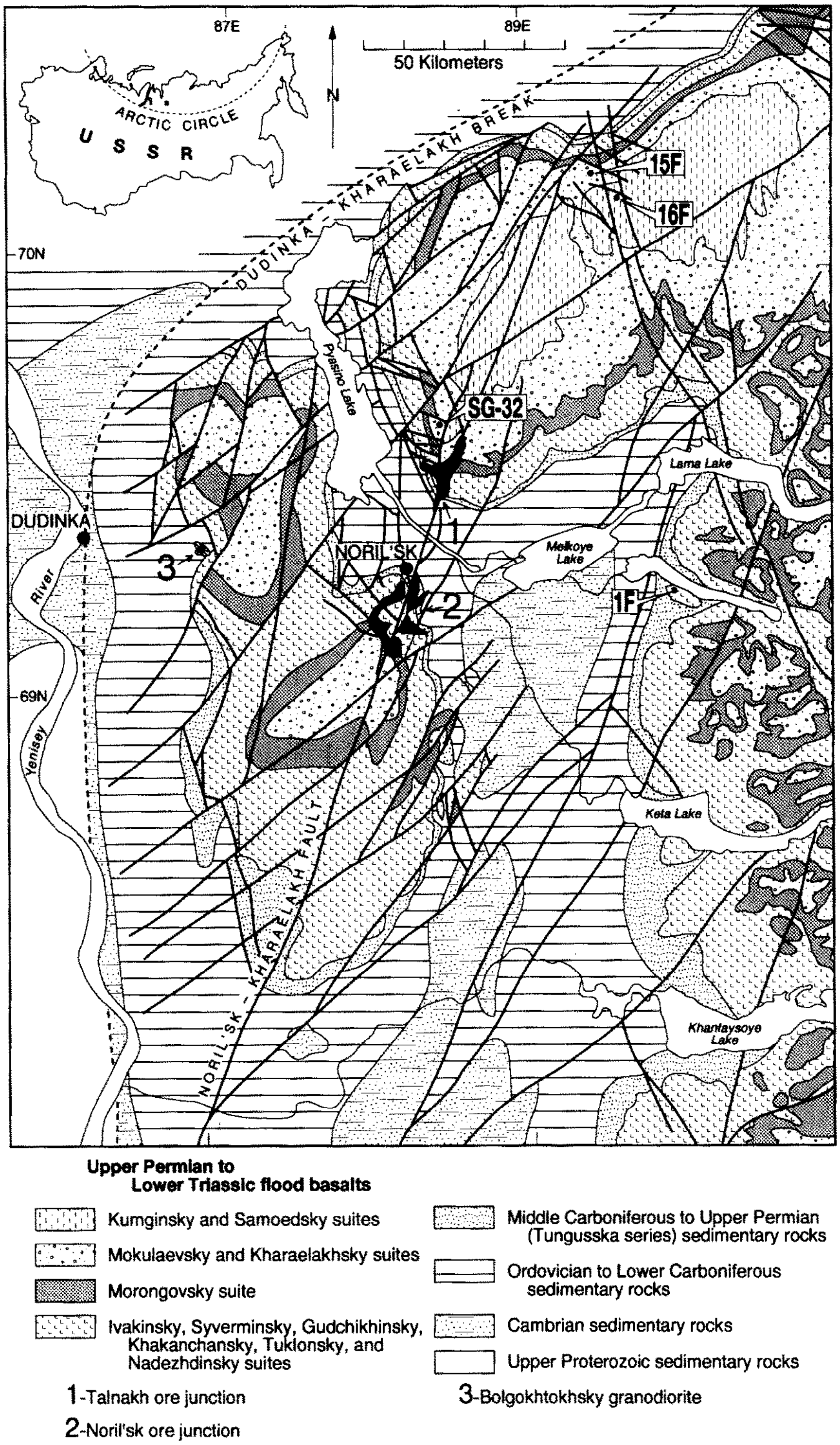

FIG. 1. Simplified geologic map of the Noril'sk area, showing major structural features, sampling locations, and subsurface outlines of the fully differentiated, ore-bearing intrusions (black, true scale).

nonrifting environment, we have chosen to embrace the plume model as an explanation for SFBP volcanism. Thus, part of this report is devoted to "testing" the plume model (e.g., CAMPBELL and GRIFFITHS, 1990) against our data set and to developing a comprehensive and credible model for the evolution of SFBP magmas. Future reports will consider the relation of the ore-bearing intrusions to the basalts on the basis of an equally extensive data set.

In this report, we sharply limit discussion of the field characteristics of the basalts and previous work on their petrographic and geochemical characteristics. The following reports, all in English, provide additional background material and analyses: FEDORENKO (1981, 1991, 1993), AL'MUKHAMEDOV and ZOLOTUKHIN (1988), ZOLOTUKHIN and AL'MUKHAMEDOV (1988, 1990, 1991), LIGHTFOOT et al. (1990b, 1993a,b), SHARMA et al. (1991, 1992), and BRÜGMANN et al. (1993). In many respects, the major- and trace-element characteristics discussed in the following text are comparable to those reported by LIGHTFOOT et al. (1990b, 1993a,b) for a comparable, but significantly less stratigraphically complete, suite of samples, many of which are from borehole SG-9, collared approximately 2.9 km S. 20°W of borehole SG-32.

FIELD, PETROGRAPHIC, AND AGE RELATIONS

The 250-Ma SFBP is one of the world's largest CFB provinces, with relatively continuous exposures of basalt covering an area of at least 3.4×10^5 km^2. MILANOVSKIY (1976) estimated that rocks associated with this early Mesozoic flood-basalt magmatism once covered an area of 4×10^6 km^2 and had a volume of $2\text{-}3 \times 10^6$ km^3. The Noril'sk area lies at the extreme northwestern corner of both the Siberian platform and the most extensive, relatively undisturbed exposures of the flood basalts. Impingement of a mantle plume beneath the margin of a Precambrian craton is most consistent with geologic and tectonic features of the SFBP, because the period 270–220 Ma was a time of continental collision and the Ural orogeny in northern Siberia (ZONENSHAIN et al., 1990). MAKARENKO (1976) and ZONENSHAIN et al. (1990) noted that rifting took place west and north of Noril'sk during the Middle to Late Triassic. We interpret the modestly extensional features noted by KUZNETSOV and NAUMOV (1975) and ZONENSHAIN et al. (1990) to be characteristic of the Noril'sk area, as responses to stretching above a rising plume head (e.g., GRIFFITHS and CAMPBELL, 1991, Fig. 13).

In the Noril'sk area, the SFBP is represented by lavas, tuffs, and intrusive rocks, with respective volume proportions of this mafic magmatism estimated at 84:10:6 (FEDORENKO, 1991). Because of the economic importance of the few, uniquely characterized ore-bearing intrusions (NALDRETT et al., 1992; ZEN'KO and CZAMANSKE, 1993), the mafic intrusions have been much studied; most are sheetlike and now compose as much as 15–20% of the sedimentary section for 2 km below the base of the basalts. About fifteen distinct types, distinguished by petrographic and geochemical characteristics, and age in relation to the lava suites, are recognized in the Noril'sk area (FEDORENKO et al., 1984; NALDRETT et al., 1992). In contrast to most other CFB provinces, SFBP activity was characterized by initial and continuing explosive volcanism; the lava:tuff volume ratio is estimated to be as high as 4:1 for the entire province. Basaltic tuffs of the first- and second-basalt assemblages typically contain 10–15 vol% of fine-grained (0.1–1 mm) minerals and lithic fragments from the underlying sedimentary rocks. Exposed within the thick basal tuff of the upper Morongovsky (Mr_2) subsuite is a diatreme (less than 6 by 14 m in surface expression) that has carried up 5–30-cm-diameter fragments of the upper crystalline basement and overlying Riphean volcanic and sedimentary rocks which lie at a depth of 9–10 km.

The thickest (>3,500 m thick) and most continuous sequence of volcanic rocks is present in the Noril'sk area (Fig. 2). This sequence is formed by alternation of lava flows (from a few meters to 100 m thick, average 15 m thick) and tuff horizons (from several tens of centimeters to 50–100-m thick, rarely 200–400 m thick). In the Noril'sk area, there are about 200 lava flows and thirty tuff horizons. Lava flows of similar composition and texture are grouped into units tens to hundreds of meters thick. Single lava and tuff units typically extend tens to hundreds of kilometers and have sharp contacts.

Lavas of the SFBP differ from the flood basalts in other provinces in their high proportion of amygdaloidal material. All of the lava flows can be divided into lower, massive and upper, amygdaloidal zones, which average 36% of the flow thickness (from 49% in the lower suites to 31% in the upper suites of the sequence). The amygdaloidal basalts that characterize the upper parts of the flows contain about 30% amygdules by volume.

Volcanic rocks commonly rest on terrigenous sedimentary rocks of the Tungusska series (C_2-P_2) above a slight unconformity; a few tens of meters to as much as 200–300 m of sedimentary rocks was eroded. In some places, Tungusska-series argillites conformably grade into SFBP tuffs, indicating that no significant uplift preceded volcanism. Beneath the Tungusska series lies a 3,700–4,700-m-thick, Cambrian through Upper Devonian sedimentary sequence containing differing proportions of dolomite, marl, limestone, argillite, anhydrite, siltstone, variegated shale, sandstone, and coal (see ZEN'KO and CZAMANSKE, 1993, Fig. 1). These sedimentary rocks rest on a Precambrian basement of schists, granitic gneisses, and granites whose age is estimated at about 2 Ga from common-lead isotopic analyses of xenoliths (J. L. Wooden, unpubl. data). At present, little is known about these crustal rocks but they are the subject of active investigation as a component of our research.

The volcanic sequence of the Noril'sk area is divided into eleven suites on the basis of the chemical composition and texture of the lavas and correlation of tuff units; seven suites are subdivided into subsuites (Fig. 2). FEDORENKO (1981) combined these suites into three basalt assemblages: (1) Ivakinsky-Gudchikhinsky, (2) Khakanchansky-Nadezhdinsky, and (3) Morongovsky-Samoedsky. Lavas of each assemblage have specific signatures of major- and trace-element chemistry. The geochemical boundary between the first two assemblages is sharp. The upper Nadezhdinsky (Nd_3) and lower Morongovsky (Mr_1) subsuites constitute a transition between the second and third assemblages. In the Noril'sk area, the Ivakinsky-Gudchikhinsky assemblage constitutes about 7%, the Khakanchansky-Nadezhdinsky assemblage about 14%, and the Morongovsky-Samoedsky assemblage the remaining 79% of the total lava volume. For the SFBP as a whole, a speculative estimate is that third-assemblage volcanic rocks constitute 90–95% of the total volume, with the remaining 5–10% divided among first-assemblage volcanic rocks (~30%), second-assemblage volcanic rocks (50–60%), and Guli volcanic rocks (10–20%). Tholeiitic basalts are dominant among SFBP lavas and are the only lava type in many areas. Alkaline and subalkaline basalts (2.5 vol%) and picritic basalts (1 vol%) are found in the Noril'sk area. Unusual lava types are characteristic of the Guli magmatic center, near the south boundary of the Yenisey-Khatanga trough, more than 500 km northeast of Noril'sk. There, trachybasalts, trachyandesitic basalts, nepheline basanites, ankaramites, high-Ti picrites, and meimechites, as well as rare dacites and rhyodacites, are present, in addition to typical SFBP basalts. The Kaltaminsky ankaramites (found in the upper part of the Morongovsky suite) and Ikonsky andesitic basalts (found in the upper part of the Kharaelakhsky suite) present in the volcanic sequence northeast of Noril'sk are related to the Guli magmatic center.

We note that SHARMA et al. (1991) appeared to imply a geographic distinction between basalts of the Noril'sk and Putorana areas, whereas SHARMA et al. (1992) more properly addressed the temporal evolution of SFBP volcanism. In general, first- and second-assemblage lavas are included in their Noril'sk-area samples, and third-assemblage lavas in their Putorana-area samples. Our report is the first to characterize an essentially continuous, well-controlled stratigraphic section through the SFBP.

Unconformities in the volcanic sequence are rare, small (a few meters of section missing), and local; traces of weathering are slight. Apparently, the topography was flat, and eruptions quickly followed one another (FEDORENKO, 1979). On the basis of paleontologic and geochemical data, FEDORENKO (1991) concluded that tuffs of the lower third of the sequence formed in water-filled basins as shallow as a few meters, whereas the upper tuffs were erupted subaerially. There is no evidence of subaqueous eruption of lava, even for the lower suites. Volcanism took place in a lowland environment that was inherited from Late Permian (Tungusska series) time, when coal-forming detritus accumulated. Lava was predominately erupted in an environment of well-compensated subsidence; some overcompensation took place later. FEDORENKO (1979, 1991) suggested that this subsidence of some 3.5 km was caused by the evacuation of magma chambers.

The depressions evident in the present tectonic structure of the SFBP (Figs. 1 and 3) formed during Late Triassic to Early Jurassic time; these include the Kharaelakh, Noril'sk, and Vologochan depressions (Fig. 3c) and the broad Tungusska basin to the southeast. During the period of volcanism, the paleostructure was simpler, and the paleodepressions were broad and gentle. Paleotectonic reconstructions allow the inference that the boundaries between the three basalt assemblages are related to two distinct periods of structural reorganization (Fig. 3; FEDORENKO, 1979, 1991). Maximal thicknesses of first-assemblage lavas are found in the north-central part, of second-assemblage lavas in the east-central part, and of third-assemblage lavas northeast of the Noril'sk area. This reorganization of the magma-supply system is reflected in geochemical distinctions between assemblages, suggesting access to different staging reservoirs and, possibly, to melts from different parts of the mantle plume.

Attempts to date the inception of flood-basalt magmatism have led to numerous conflicting ages in the range 254–238 Ma. In an attempt using the $^{40}Ar/^{39}Ar$ laser age-spectrum technique, DALRYMPLE et al. (1991) obtained an age of 249 $\pm$ 1.6 (2σ) Ma on biotite from a mineralized vein in the ore-bearing Noril'sk I intrusion, in comparison with an apparent age of 244.9 $\pm$ 1.8 Ma on plagioclase from basalt sample SG-32-2515.4 of the Syverminsky suite that is cut by this intrusion. On the basis of this and comparable ages for other basalt samples (see CAMPBELL et al., 1992), they concluded that the Siberian flood basalts dated by them have lost about 2% of their radiogenic argon. Subsequently, Dalrymple et al. (unpubl. data) obtained an $^{40}Ar/^{39}Ar$ age of 248.9 $\pm$ 2.8 for the Lower Talnakh intrusion, and CAMPBELL et al. (1992) obtained a U-Pb age of 248 $\pm$ 4 Ma for the Noril'sk I intrusion, based on SHRIMP ion-microprobe dating of zircon extracted from a sample of taxitic leucogabbro collected in the Medvezhy Creek open-pit mine of the Noril'sk I intrusion. The combined results of this and earlier studies (e.g., FEDORENKO et al., 1984; LIGHTFOOT et al., 1990b, 1993a) suggest that the Noril'sk I intrusion may be related in time to eruption of the thick tuff unit at the base of the Mr_2 subsuite (Fig. 2), a midpoint in the volcanic sequence.

Inasmuch as the ages obtained for the Noril'sk I intrusion are not statistically different from the age of 251.1 $\pm$ 3.6 Ma recently determined by SHRIMP for the Permian-Triassic boundary (CLAQUÉ-LONG et al., 1991), CAMPBELL et al. (1992) argued that eruption of the Siberian flood basalts may have contributed to the Permian-Triassic extinction event. The magnetostratigraphy of the late Permian and early Triassic (e.g., HAAG and HELLER, 1991) and the fact that all but the Ivakinsky suite are normally polarized (LIND and SCHEKOTUROV, 1991) lead to the inference that the entire SFBP was formed in about 600,000 years (CAMPBELL et al., 1992; CZAMANSKE et al., 1992a).

SAMPLE SELECTION, PREPARATION, AND ANALYSIS

The fifty-three samples reported on here were chosen on the basis of trace-element chemistry from our larger set of seventy-nine samples of the SFBP in the Noril'sk area. Most of the samples are from borehole SG-32, which penetrated 2,640 m of the lower suites of the SFBP (Figs. 1 and 2); for these samples, the final digits in the sample designation represent the depth in the borehole in meters. Supplementary samples were collected from surface outcrops at four localities (Fig. 1) to complete stratigraphic coverage of all eleven basalt suites and their subsuites (Fig. 2). This stratigraphic coverage is from within 44 m of the top of the basalt sequence at locality 16F to within 15 m of the SFBP-Tungusska series contact in borehole SG-32. Sample Mik-1 is clinopyroxene spinifex from a 45–86 m thick, differentiated flow exposed along the Mikchanda River (DODIN and GOLUBKOV, 1971; RYABOV et al., 1977).

Where present, weathered rinds were sawed or ground from all outcrop samples. All sawn surfaces and the circumference of all core samples were ground free of striations on a sintered-metal lap impregnated with 100-mesh diamonds. Samples were passed twice through a successively constrained iron-jawed crusher and reduced to powder in an alumina-lined shatterbox. Many of the samples are considerably altered (Table 1; data for H_2O^+ and CO_2). For the borehole samples, this alteration is unrelated to the present erosional surface and, for the first and second assemblages, may in part be due to emplacement of the subjacent ore-bearing intrusions. Rare secondary-alteration veinlets and evident amygdules were removed during sample preparation. We are acutely aware that alteration could be responsible for some of the geochemical and isotopic variations that we document, but we do not believe that it compromises our principal conclusions.

Major elements were determined by X-ray fluorescence; Ba, Cu, Cr, Ni, Rb, Sr, Zn, and Zr were determined by energy-dispersive X-ray fluorescence; rare earth elements (REEs) and the rest of the minor elements were determined by instrumental neutron activation; and lead was determined by isotope-dilution mass spectrometry. The major- and trace-element data presented were produced by a team effort and represent the best obtainable from the USGS laboratories. Analytical uncertainties in these techniques, as applied in the USGS,

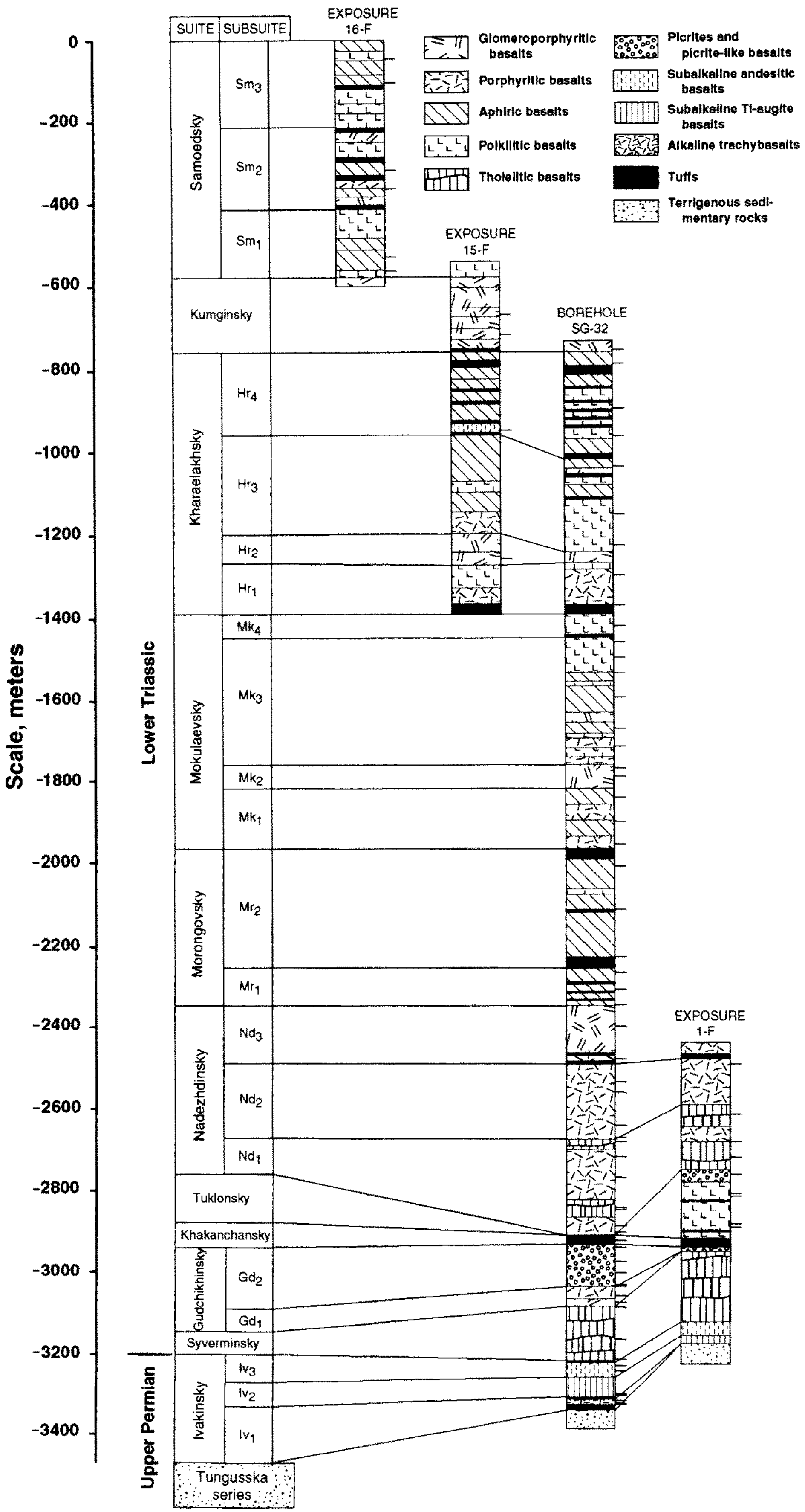

FIG. 2. Composite stratigraphic section showing the petrography of the basalts in the Noril'sk area and their classification into suites and subsuites. Distribution of 78 samples shown by ticks to the right of the columns.

Table 1. Major-element, trace-element and isotopic data for the SFBP basalts of the Noril'sk area.

Sample no.	16F-19	16F-17	16F-2	15F-36	SG-32 54	SG-32 87	SG-32 196	15F-25	SG-32 260.5	SG-32 524.5	SG-32 670	SG-32 719	SG-32 799
Suite	Sm_3	Sm_3	Sm_1	Km	Km	Hr_4	Hr_4	Hr_4	Hr_4	Hr_3	Hr_1	Mk_4	Mk_3
Depth, m	-44	-94	-565	-672	-754	-787	-896	-952	-961	-1225	-1370	-1419	-1499
SiO_2	49.41	49.92	49.25	49.67	49.60	49.31	49.39	54.90	48.80	49.24	49.45	47.76	49.74
Al_2O_3	15.16	15.15	15.35	15.42	15.61	15.30	15.23	14.12	15.54	15.86	15.43	16.41	15.58
FeOT	12.34	11.94	11.95	12.28	12.28	12.55	12.65	11.67	12.30	11.93	12.40	12.48	12.42
MgO	7.29	7.37	7.67	6.63	6.52	6.77	6.68	3.92	7.80	7.59	7.40	7.36	6.83
CaO	11.55	11.21	11.64	11.49	11.40	11.27	11.63	7.66	11.40	11.09	10.93	12.07	11.01
Na_2O	2.25	2.12	2.16	2.34	2.38	2.32	2.23	2.97	2.07	2.14	2.24	2.09	2.30
K_2O	0.18	0.56	0.22	0.24	0.25	0.51	0.14	1.77	0.42	0.48	0.39	0.11	0.30
TiO_2	1.45	1.38	1.38	1.52	1.55	1.58	1.62	2.31	1.32	1.33	1.41	1.36	1.45
P_2O_5	0.17	0.16	0.18	0.21	0.21	0.21	0.21	0.52	0.15	0.16	0.15	0.16	0.17
MnO	0.21	0.20	0.21	0.21	0.21	0.19	0.22	0.16	0.21	0.20	0.20	0.21	0.20
H_2O+	1.68	2.07	0.78	1.10	1.94	1.96	1.50	1.01	1.71	1.47	1.01	1.41	1.19
H_2O-	0.80	1.18	1.62	1.92	0.42	0.75	3.53	1.52	1.57	1.68	0.67	3.41	1.86
CO_2	0.01	0.03	0.04	0.03	0.01	0.18	0.10	0.14	0.05	0.04	0.03	0.10	0.03
S	<0.01	<0.01	<0.01	<0.01	<0.01	<0.01	<0.01	<0.01	<0.01	<0.01	<0.01	<0.01	<0.01
Ba, ppm	120	149	124	130	140	163	84	550	141	112	123	68	145
Cr	182	181	216	100	113	112	70	30	164	160	123	131	71
Cs	0.18	0.09	0.00	0.39	0.48	-	<.06	0.37	<.2	0.18	0.28	-	0.31
Hf	2.71	2.62	2.53	2.89	3.19	3.14	2.93	6.93	2.25	2.32	2.43	2.52	2.71
Nb	10	8	8	8	12	8	11	27	13	10	7	13	14
Pb	1.90	1.70	1.74	2.33	2.46	2.53	2.80	7.11	1.25	1.54	1.61	1.49	1.82
Rb	8	10	4	9	8	9	6	46	10	8	14	2	5
Sc	38	37	38	38	36	38	37	23	39	36	37	40	37
Sr	194	201	181	195	205	190	186	394	164	178	180	178	204
Ta	0.282	0.271	0.281	0.355	0.380	0.377	0.330	1.495	0.223	0.229	0.264	0.280	0.300
Th	1.021	1.033	1.072	1.418	1.540	1.582	1.311	4.515	0.752	0.854	0.880	1.010	1.111
U	0.396	0.401	0.534	0.783	0.761	0.819	0.665	1.142	0.328	0.436	0.303	0.355	0.402
Y	33	28	29	32	38	38	32	43	29	27	36	31	27
Zn	78	98	81	87	75	93	77	93	86	98	75	91	73
Zr	113	106	117	128	133	132	133	311	98	101	104	105	114
Co, ppm	51	51	51	48	46	50	48	29	54	53	50	53	50
Cu	107	178	159	130	111	170	180	56	128	135	166	148	147
Ni	126	145	146	106	103	122	116	30	164	176	137	155	137
Pt, ppb	12.4	13.5	10.3	11.4	12.3	14.5	13.7	2.1	11.4	10.4	13.3	11.6	11.4
Pd	9.9	9.3	9.7	11.4	17.5	14.5	16.9	3.6	10.4	13.5	17.4	10.6	10.4
La, ppm	8.28	8.00	7.94	10.01	9.59	10.34	9.32	34.5	5.91	6.62	7.02	7.77	8.46
Ce	20.8	19.8	18.5	23.4	25.0	25.2	21.4	79.8	14.1	15.7	17.4	19.6	21.2
Nd	13.72	12.56	10.61	14.80	15.20	15.40	14.17	46.5	9.58	10.68	11.54	12.81	13.19
Sm	3.88	3.58	3.69	4.22	4.25	4.21	4.22	10.48	3.26	3.37	3.53	3.59	3.87
Eu	1.32	1.23	1.23	1.33	1.42	1.37	1.34	2.92	1.16	1.16	1.21	1.23	1.25
Gd	4.70	4.19	4.36	4.59	4.95	5.25	5.12	10.15	4.15	4.14	4.24	3.94	4.60
Tb	0.797	0.729	0.734	0.805	0.851	0.875	0.829	1.463	0.715	0.712	0.702	0.669	0.724
Ho	1.114	1.034	1.072	1.180	1.191	1.241	1.195	1.702	1.067	1.047	0.995	0.966	1.025
Tm	0.461	0.442	0.455	0.523	0.499	0.516	0.505	0.618	0.453	0.440	0.438	0.431	0.437
Yb	2.88	2.72	2.77	3.30	3.11	3.25	3.21	3.61	2.78	2.79	2.76	2.75	2.73
Lu	0.442	0.399	0.414	0.478	0.464	0.479	0.472	0.513	0.414	0.391	0.414	0.415	0.419
$\frac{^{232}Th}{^{204}Pb}$	35.05	39.45	40.37	39.96	41.03	40.99	30.57	40.87	39.26	36.13	35.61	44.25	39.87
$\frac{^{238}U}{^{204}Pb}$	13.25	14.92	19.60	21.53	19.76	20.68	15.12	10.08	16.71	17.99	11.98	15.15	14.06
$\left(\frac{^{206}Pb}{^{204}Pb}\right)_M$	18.288	18.231	18.684	18.770	18.844	18.840	18.568	17.630	18.570	18.453	18.466	18.459	18.347
$\left(\frac{^{206}Pb}{^{204}Pb}\right)_I$	17.764	17.641	17.909	17.919	18.063	18.022	17.970	17.231	17.909	17.741	17.992	17.860	17.791
$\left(\frac{^{207}Pb}{^{204}Pb}\right)_M$	15.487	15.465	15.514	15.516	15.505	15.511	15.508	15.440	15.508	15.499	15.502	15.509	15.482
$\left(\frac{^{207}Pb}{^{204}Pb}\right)_I$	15.460	15.435	15.474	15.472	15.465	15.469	15.477	15.419	15.474	15.463	15.478	15.478	15.453
$\left(\frac{^{208}Pb}{^{204}Pb}\right)_M$	38.159	38.096	38.249	38.197	38.148	38.136	38.077	37.985	38.177	38.180	38.199	38.244	38.168
$\left(\frac{^{208}Pb}{^{204}Pb}\right)_I$	37.723	37.605	37.746	37.700	37.637	37.626	37.696	37.477	37.689	37.731	37.756	37.693	37.672
$\left(\frac{^{87}Sr}{^{86}Sr}\right)_M$	0.70506	0.70525	0.70511	0.70516	0.70510	0.70522	0.70494	0.70698	0.70479	0.70512	0.70542	0.70521	0.70542
$\left(\frac{^{87}Sr}{^{86}Sr}\right)_I$	0.70462	0.70472	0.70488	0.70467	0.70469	0.70472	0.70459	0.70579	0.70414	0.70464	0.70460	0.70509	0.70516

Sample no.	SG-32 1070	SG-32 1203	SG-32 1255	SG-32 1311	SG-32 1415	SG-32 1528	SG-32 1645	SG-32 1701	SG-32 1782	SG-32 1838	SG-32 1970	SG-32 1982	SG-32 2069
Suite	Mk_2	Mk_1	Mk_1	Mr_2	Mr_2	Mr_2	Mr_1	Nd_3	Nd_3	Nd_2	Nd_2	Nd_1	Nd_1
Depth, m	-1770	-1903	-1955	-2011	-2115	-2228	-2345	-2401	-2482	-2538	-2670	-2682	-2769
SiO_2	49.41	49.90	49.79	49.71	49.64	49.67	49.99	50.55	50.84	52.87	52.96	51.44	53.67
Al_2O_3	15.70	15.46	15.39	15.41	15.66	15.39	15.73	15.81	15.43	15.08	15.15	15.23	15.29
FeOT	11.67	11.57	11.43	10.99	11.58	11.72	10.58	10.57	10.61	10.17	9.69	9.57	9.60
MgO	6.83	6.80	7.10	7.85	7.41	7.49	7.59	6.62	6.93	6.43	6.79	7.32	6.38
CaO	12.67	12.35	12.50	12.22	11.74	11.49	12.39	12.17	11.80	10.59	10.77	10.64	10.02
Na_2O	2.03	2.17	2.11	2.02	2.08	2.18	2.03	2.34	2.25	2.28	2.25	2.49	2.32
K_2O	0.10	0.22	0.12	0.38	0.36	0.47	0.25	0.58	0.62	1.17	1.14	2.12	1.42
TiO_2	1.25	1.21	1.21	1.09	1.19	1.24	1.11	0.98	1.15	1.09	0.97	0.90	0.99
P_2O_5	0.16	0.16	0.15	0.14	0.14	0.15	0.15	0.22	0.17	0.14	0.13	0.11	0.14
MnO	0.19	0.18	0.20	0.18	0.20	0.19	0.18	0.17	0.20	0.17	0.16	0.17	0.17
H_2O+	1.50	1.26	1.13	1.20	1.78	1.36	0.19	1.34	1.31	0.96	0.50	3.32	1.87
H_2O-	2.62	1.63	1.80	1.13	0.56	0.38	3.49	1.99	1.71	1.02	0.67	0.51	0.69
CO_2	0.04	0.03	0.04	0.04	0.09	0.17	0.05	0.07	0.04	0.05	1.04	0.24	0.10
S	0.01	<0.01	<0.01	<0.01	<0.01	<0.01	<0.01	<0.01	<0.01	0.01	0.03	< 0.01	< 0.01
Ba, ppm	90	124	86	144	146	152	158	296	223	331	285	762	380
Cr	119	112	105	191	126	162	75	116	99	28	106	72	127
Cs	0.17	0.40	0.37	0.12	0.54	0.11	0.21	0.18	2.59	0.30	1.26	0.46	0.70
Hf	2.25	2.36	2.22	2.01	2.44	2.43	2.42	2.59	2.83	3.44	3.07	2.61	3.28
Nb	4	9	5	10	8	8	7	12	14	12	15	4	14
Pb	1.65	1.99	2.07	1.55	2.49	2.12	2.54	3.40	3.11	5.70	4.94	2.13	12.37
Rb	4	4	5	9	7	12	4	11	13	23	37	88	38
Sc	37	39	37	38	39	39	34	35	36	32	30	30	30
Sr	215	228	222	205	216	205	229	322	249	250	239	402	262
Ta	0.269	0.288	0.274	0.258	0.301	0.291	0.338	0.400	0.415	0.583	0.501	0.427	0.627
Th	0.989	1.089	1.054	0.894	1.226	1.252	1.729	2.111	2.143	3.504	3.182	2.807	3.838
U	0.407	0.428	0.487	0.419	0.496	0.487	0.668	1.082	0.857	1.110	0.994	0.815	1.139
Y	23	26	25	25	31	35	26	33	31	28	27	19	30
Zn	93	75	84	105	87	101	106	106	69	92	84	90	93
Zr	93	96	93	85	103	108	108	119	133	141	130	109	142
Co, ppm	47	50	48	48	51	49	46	41	46	43	41	40	38
Cu	151	124	136	98	142	64	69	30	135	81	75	10	26
Ni	113	122	132	148	142	140	115	108	104	50	53	24	24
Pt, ppb	11.5	10.4	9.9	11.3	15.4	11.3	7.7	2.1	8.1	<.5	<.5	<.5	<.5
Pd	10.4	11.4	11.4	9.6	13.4	10.0	3.2	2.0	8.5	<.5	<.5	<.5	<.5
La, ppm	7.23	7.91	7.45	6.51	8.38	8.90	10.73	14.46	13.15	18.8	17.1	16.7	19.9
Ce	18.1	19.9	18.1	16.3	19.8	20.7	24.5	32.3	28.9	41.1	37.3	34.7	44.1
Nd	12.46	12.76	11.67	10.09	12.67	12.72	14.37	16.02	15.64	18.8	17.6	17.0	20.8
Sm	3.42	3.52	3.31	2.98	3.44	3.43	3.57	3.75	3.98	4.54	4.03	3.80	4.60
Eu	1.10	1.14	1.06	1.02	1.13	1.15	1.09	1.06	1.13	1.18	1.07	1.04	1.16
Gd	3.93	4.15	3.69	3.57	3.81	4.06	3.94	3.99	4.51	4.77	3.95	3.82	4.63
Tb	0.613	0.666	0.592	0.617	0.656	0.697	0.637	0.654	0.724	0.729	0.652	0.596	0.703
Ho	0.862	0.949	0.860	0.905	0.990	1.036	0.891	0.997	0.989	1.121	0.929	0.793	0.993
Tm	0.408	0.411	0.381	0.374	0.417	0.432	0.359	0.474	0.431	0.417	0.370	-	-
Yb	2.46	2.56	2.40	2.33	2.66	2.75	2.20	3.05	2.72	2.57	2.30	1.99	2.50
Lu	0.362	0.373	0.352	0.340	0.383	0.404	0.331	0.459	0.384	0.378	0.352	0.297	0.355
$\frac{^{232}Th}{^{204}Pb}$	39.21	35.81	33.43	37.83	32.36	38.64	44.52	40.76	45.16	39.88	41.82	86.78	20.08
$\frac{^{238}U}{^{204}Pb}$	15.73	13.73	15.05	17.29	12.78	14.66	16.76	20.36	17.61	12.32	12.74	24.56	5.81
$\left(\frac{^{206}Pb}{^{204}Pb}\right)_M$	18.623	18.588	18.625	18.765	18.759	18.677	18.514	18.903	18.533	18.083	18.089	18.524	17.940
$\left(\frac{^{206}Pb}{^{204}Pb}\right)_I$	18.001	18.045	18.030	18.081	18.254	18.097	17.851	18.099	17.836	17.596	17.585	17.552	17.711
$\left(\frac{^{207}Pb}{^{204}Pb}\right)_M$	15.525	15.522	15.529	15.527	15.581	15.516	15.511	15.541	15.508	15.491	15.489	15.521	15.482
$\left(\frac{^{207}Pb}{^{204}Pb}\right)_I$	15.493	15.494	15.499	15.492	15.555	15.486	15.477	15.500	15.472	15.466	15.463	15.471	15.470
$\left(\frac{^{208}Pb}{^{204}Pb}\right)_M$	38.242	38.200	38.233	38.210	38.337	38.197	38.235	38.067	38.237	38.113	38.124	38.632	37.996
$\left(\frac{^{208}Pb}{^{204}Pb}\right)_I$	37.754	37.755	37.817	37.740	37.934	37.716	37.681	37.559	37.674	37.617	37.603	37.552	37.747
$\left(\frac{^{87}Sr}{^{86}Sr}\right)_M$	0.70547	0.70559	0.70565	0.70555	0.70552	0.70565	0.70643	0.70660	0.70697	0.70946	0.71030	0.71088	0.71021
$\left(\frac{^{87}Sr}{^{86}Sr}\right)_I$	0.70527	0.70540	0.70541	0.70508	0.70518	0.70503	0.70624	0.70623	0.70641	0.70849	0.70872	0.70822	0.70872

Table 1. Major-element, trace-element and isotopic data for the SFBP basalts of the Noril'sk area.–(Continued)

Sample no.	SG-32 2144.3	SG-32 2149.8	SG-32 2212.5	1F-32	1F-30	1F-27	1F-25	1F-22	Mik-1	SG-22 2226.7	SG-32 2245.5	SG-32 2275.6	SG-32 2301	SG-32 2328
Suite	Nd_1	Nd_1	Nd_1	Tk	Tk	Tk	Tk	Tk	Tk	Hk	Gd_2	Gd_2	Gd_2	Gd_2
Depth, m	-2844	-2850	-2913	-2922	-2932	-2972	-2982	-3056		-3097	-3116	-3146	-3171	-3198
SiO_2	53.06	52.33	53.48	47.65	47.79	49.88	49.68	49.94	51.92	52.72	48.41	49.47	48.53	49.08
Al_2O_3	15.05	15.36	15.25	12.15	12.73	15.67	15.78	15.71	9.23	15.09	8.72	11.08	9.73	10.05
FeOT	9.38	9.67	9.26	11.59	11.15	10.19	9.81	10.10	6.37	9.34	13.75	12.86	13.06	12.87
MgO	7.54	7.19	6.82	16.7	16.5	9.19	8.81	9.51	13.51	7.08	18.2	14.0	13.2	17.1
CaO	8.95	10.75	9.41	9.15	9.41	11.75	12.82	10.82	16.97	10.35	7.96	7.69	12.11	8.00
Na_2O	2.80	2.31	2.75	1.29	1.10	1.89	1.80	2.42	0.86	2.26	1.10	2.95	1.44	1.10
K_2O	2.03	1.14	1.82	0.41	0.31	0.20	0.10	0.33	0.61	1.92	0.09	0.05	0.18	0.05
TiO_2	0.91	0.96	0.92	0.79	0.73	0.95	0.93	0.92	0.39	0.90	1.43	1.61	1.43	1.45
P_2O_5	0.12	0.12	0.12	0.08	0.09	0.11	0.10	0.08	<.05	0.13	0.12	0.14	0.14	0.12
MnO	0.17	0.16	0.16	0.18	0.18	0.17	0.16	0.17	0.14	0.21	0.20	0.17	0.18	0.17
H_2O+	3.39	1.34	1.82	3.70	4.88	1.62	1.88	2.98	0.97	4.26	3.87	3.95	2.82	4.50
H_2O-	0.67	0.58	0.59	1.30	1.08	3.07	3.12	0.41	0.47	1.23	2.70	2.02	2.72	2.70
CO_2	0.50	0.20	0.22	0.11	0.11	0.07	0.19	0.05	0.17	6.82	0.87	0.47	2.84	0.22
S	<0.01	<0.01	<0.01	<0.01	<0.01	<0.01	0.01	0.01	<0.01	0.05	<0.01	<0.01	<0.01	<0.01
Ba, ppm	884	353	376	127	116	208	148	101	136	326	35	27	57	19
Cr	247	172	268	581	831	387	318	395	2337	366	847	828	880	721
Cs	0.28	0.64	0.53	2.34	4.88	0.05	-	-	0.16	2.60	3.35	0.42	1.66	1.44
Hf	2.80	2.89	2.97	1.36	1.40	1.60	1.55	1.53	0.82	2.41	2.14	2.54	2.17	2.13
Nb	13	12	7	8	11	6	10	11	6	14	16	12	14	4
Pb	2.01	5.00	3.83	0.81	0.80	1.43	1.76	1.26	0.91	6.94	0.61	1.24	1.44	1.08
Rb	61	29	62	12	13	3	3	14	12	57	13	4	6	6
Sc	32	33	32	29	30	34	37	38	58	25	23	26	23	25
Sr	337	271	335	175	138	270	275	276	290	215	150	187	187	140
Ta	0.459	0.458	0.455	0.148	0.169	0.199	0.177	0.173	0.117	0.422	0.404	0.477	0.404	0.391
Th	3.063	2.929	2.885	0.529	0.525	0.683	0.603	0.648	0.601	2.824	0.856	1.172	0.930	0.912
U	0.748	0.668	0.714	0.150	0.206	0.196	0.123	0.140	0.207	0.989	0.390	0.465	0.344	0.367
Y	25	28	21	12	16	17	21	24	12	29	24	19	25	15
Zn	89	92	84	75	73	51	72	87	51	114	119	116	110	112
Zr	131	131	124	58	57	75	69	67	37	114	92	99	91	80
Co, ppm	40	42	41	83	82	52	50	52	40	40	93	70	80	83
Cu	31	56	103	76	56	101	100	127	21	126	122	153	125	56
Ni	41	54	76	365	383	157	133	158	56	135	1031	634	825	764
Pt, ppb	0.7	<.5	5.2	10.6	12.9	9.3	7.3	8.9	<.5	6.5	14.1	11.8	9.6	14.0
Pd	<.5	<.5	3.0	6.8	6.3	9.3	9.3	13.5	<.5	7.9	8.7	9.9	7.5	9.8
La, ppm	16.6	16.9	16.28	4.80	5.13	7.06	6.37	5.06	4.68	18.9	6.74	6.96	6.94	6.71
Ce	34.0	34.3	37.3	11.41	11.87	17.6	15.36	12.07	10.97	36.0	18.3	20.0	16.8	18.0
Nd	15.69	17.8	18.1	6.88	7.55	8.83	8.63	8.08	6.82	17.5	12.05	13.66	12.21	11.30
Sm	3.52	3.91	3.96	1.94	2.02	2.56	2.46	2.33	1.81	3.84	3.21	3.85	3.43	3.25
Eu	1.06	1.12	1.07	0.71	0.74	0.93	1.01	0.90	0.54	1.00	1.03	1.25	1.08	1.12
Gd	3.84	3.75	3.74	2.37	2.43	2.92	2.85	2.77	1.99	3.98	3.61	4.10	3.82	3.44
Tb	0.613	0.625	0.597	0.386	0.392	0.477	0.466	0.493	0.292	0.605	0.545	0.619	0.556	0.564
Ho	0.781	0.884	0.839	0.523	0.548	0.651	0.625	0.696	0.416	0.762	0.689	0.733	0.682	0.696
Tm	0.313	0.355	0.343	-	0.231	-	0.274	0.289	-	0.316	0.239	-	0.234	0.242
Yb	1.99	2.25	2.12	1.41	1.42	1.69	1.75	1.63	1.12	2.00	1.39	1.54	1.38	1.41
Lu	0.314	0.326	0.308	0.205	0.211	0.250	0.267	0.274	0.158	0.300	0.189	0.208	0.194	0.197
$\frac{^{232}Th}{^{204}Pb}$	101.15	38.08	48.59	41.46	41.97	30.66	21.91	33.49	42.69	26.62	93.49	62.47	42.36	55.80
$\frac{^{238}U}{^{204}Pb}$	24.09	8.46	11.72	11.46	16.04	8.57	4.36	7.07	14.34	9.09	41.47	24.13	15.29	21.90
$\left(\frac{^{206}Pb}{^{204}Pb}\right)_M$	18.742	18.056	17.796	17.462	17.449	17.627	17.588	18.152	18.036	18.490	19.117	18.856	18.738	18.865
$\left(\frac{^{206}Pb}{^{204}Pb}\right)_I$	17.79	17.721	17.333	17.009	16.815	17.288	17.415	17.872	17.468	18.130	17.477	17.902	18.133	18.000
$\left(\frac{^{207}Pb}{^{204}Pb}\right)_M$	15.533	15.480	15.443	15.419	15.425	15.432	15.414	15.502	15.478	15.525	15.616	15.616	15.588	15.593
$\left(\frac{^{207}Pb}{^{204}Pb}\right)_I$	15.484	15.463	15.419	15.396	15.392	15.414	15.405	15.488	15.449	15.507	15.532	15.568	15.557	15.549
$\left(\frac{^{208}Pb}{^{204}Pb}\right)_M$	39.050	38.211	38.026	37.459	37.515	37.770	37.573	38.157	38.150	38.235	38.559	38.313	38.194	38.295
$\left(\frac{^{208}Pb}{^{204}Pb}\right)_I$	37.791	37.737	37.421	36.943	36.993	37.389	37.300	37.740	37.619	37.904	37.395	37.535	37.667	37.600
$\left(\frac{^{87}Sr}{^{86}Sr}\right)_M$	0.71003	0.70852	0.70957	0.70636	0.70649	0.70612	0.70602	0.70578	0.70875	0.70993	0.70660	0.70697	0.70651	0.70647
$\left(\frac{^{87}Sr}{^{86}Sr}\right)_I$	0.70816	0.70743	0.70767	0.70568	0.70553	0.70600	0.70590	0.70528	0.70832	0.70719	0.70571	0.70673	0.70621	0.70600

Sample no.	SG-32 2332.7	SG-32 2357.5	SG-32 2375.2	SG-32 2386.2	SG-32 2464.8	SG-32 2515.4	SG-32 2533.7	SG-32 2543.9	SG-32 2597.1	SG-32 2605	SG-32 2616	SG-32 2622	SG-32 2624.6
Suite	Gd_2	Gd_1	Gd_1	Sv	Sv	Sv	Iv_3	Iv_3	Iv_2	Iv_2	Iv_1	Iv_1	Iv_1
Depth, m	-3203	-3228	-3245	-3256	-3335	-3385	-3404	-3414	-3467	-3475	-3486	-3492	-3495
SiO_2	48.17	50.73	49.74	49.61	53.15	52.59	53.60	53.77	52.15	51.06	47.13	47.73	47.20
Al_2O_3	10.32	14.00	18.00	15.73	15.51	15.58	14.76	14.07	14.57	15.69	15.64	15.87	14.92
FeOT	13.51	12.68	9.19	11.86	10.08	9.96	11.77	13.78	12.72	13.62	15.41	15.24	13.50
MgO	16.1	7.06	6.64	6.28	7.09	5.95	5.19	2.87	3.81	4.42	4.62	5.36	4.03
CaO	8.74	8.11	9.91	9.91	6.79	10.12	5.76	4.96	7.88	5.29	7.13	4.51	9.45
Na_2O	1.24	3.76	3.41	3.52	3.98	2.84	3.45	3.00	3.38	4.57	3.27	4.62	3.41
K_2O	0.07	0.85	1.37	0.46	1.34	0.76	2.67	3.53	1.84	1.84	1.43	1.27	2.33
TiO_2	1.49	2.37	1.44	2.14	1.66	1.80	2.25	2.58	2.55	2.41	3.82	3.89	3.66
P_2O_5	0.14	0.22	0.17	0.32	0.23	0.25	0.36	1.13	0.88	0.78	1.35	1.37	1.26
MnO	0.17	0.21	0.14	0.16	0.16	0.15	0.19	0.32	0.22	0.32	0.20	0.12	0.24
H_2O+	4.04	2.96	2.43	3.68	2.92	1.40	2.57	2.08	1.45	3.00	3.77	4.42	2.50
H_2O-	3.29	0.81	0.45	0.81	0.90	2.32	1.09	1.23	2.62	0.77	0.82	0.95	0.76
CO_2	0.46	0.57	0.50	0.10	0.17	0.16	0.08	0.09	0.25	0.49	2.19	1.75	1.60
S	<0.01	<0.01	<0.01	<0.01	<0.01	<0.01	0.03	0.04	0.02	<0.01	<0.01	0.04	0.11
Ba, ppm	34	221	375	70	388	361	691	1470	929	937	561	870	1164
Cr	741	95	255	164	225	163	96	11	11	11	11	22	11
Cs	1.79	0.31	0.81	0.05	0.16	0.85	0.53	1.18	0.95	0.88	0.59	0.32	3.30
Hf	2.17	3.69	2.35	4.50	4.50	4.37	6.91	8.60	8.56	5.39	7.84	7.90	7.10
Nb	23	18	10	19	20	15	29	34	34	23	38	45	44
Pb	0.66	1.89	1.87	1.30	2.44	3.71	5.28	14.26	10.63	3.74	6.42	5.15	7.88
Rb	5	27	42	11	40	10	82	67	25	42	35	22	51
Sc	24	25	23	29	22	25	25	24	22	22	23	24	22
Sr	172	379	937	179	493	429	628	446	449	516	367	261	386
Ta	0.438	0.745	0.408	0.779	0.941	0.864	1.528	1.806	1.668	1.327	2.405	2.512	2.254
Th	0.942	1.979	0.657	2.438	3.638	3.147	5.842	7.204	4.867	3.643	6.309	6.230	5.788
U	0.340	0.427	0.158	0.604	0.968	0.809	1.560	1.817	1.267	1.158	3.236	2.272	2.317
Y	24	36	23	36	29	27	46	57	56	41	55	57	59
Zn	113	137	79	112	90	90	101	111	158	112	98	70	167
Zr	101	162	112	222	215	199	309	410	422	232	394	402	386
Co, ppm	80	46	41	41	39	38	34	26	26	33	38	49	38
Cu	105	103	69	35	39	31	38	32	32	19	37	35	48
Ni	818	147	103	64	111	56	46	23	32	60	54	45	39
Pt, ppb	12.0	6.1	<.5	<.5	<.5	<.5	<.5	<.5	<.5	<.5	<.5	<.5	<.5
Pd	7.3	2.8	<.5	<.5	<.5	<.5	<.5	<.5	<.5	<.5	<.5	<.5	<.5
La, ppm	6.74	12.31	9.18	25.8	26.4	22.0	45.5	61.9	50.7	38.6	53.5	51.5	50.7
Ce	18.3	30.7	20.5	49.0	52.9	48.0	92.8	134	111	92.1	121	119	109
Nd	13.08	19.1	13.11	24.8	26.2	24.5	43.1	66.2	56.5	47.8	57.7	56.6	52.6
Sm	3.40	5.12	3.32	5.74	5.64	5.37	8.30	13.65	11.72	10.44	11.65	11.53	10.39
Eu	1.11	1.79	1.30	1.87	1.73	1.81	2.26	3.86	3.52	2.64	2.93	2.74	2.95
Gd	3.75	5.58	3.25	5.73	5.55	5.71	7.69	12.60	11.61	9.99	10.39	10.59	9.51
Tb	0.569	0.875	0.576	0.884	0.868	0.871	1.235	1.890	1.731	1.411	1.531	1.555	1.492
Ho	0.627	1.044	0.675	1.161	1.090	1.140	1.581	2.363	2.185	1.685	2.038	1.979	1.989
Tm	-	0.363	0.259	0.441	0.425	0.432	0.588	0.773	0.747	0.628	0.768	0.608	0.746
Yb	1.38	2.13	1.54	2.62	2.45	2.53	3.70	4.73	4.60	3.84	4.78	4.84	4.48
Lu	0.190	0.299	0.219	0.375	0.345	0.349	0.518	0.670	0.646	0.536	0.699	0.707	0.646
$\frac{^{232}Th}{^{204}Pb}$	93.53	68.85	22.67	124.38	98.21	55.39	72.13	32.82	29.60	63.27	65.21	79.83	48.29
$\frac{^{238}U}{^{204}Pb}$	32.92	14.49	5.32	30.02	25.46	13.88	18.77	8.07	7.51	19.61	32.60	28.38	18.84
$\left(\frac{^{206}Pb}{^{204}Pb}\right)_M$	18.951	18.545	18.010	18.675	18.468	18.244	18.235	18.017	17.865	18.134	19.168	18.928	18.914
$\left(\frac{^{206}Pb}{^{204}Pb}\right)_I$	17.649	17.972	17.799	17.488	17.461	17.695	17.493	17.698	17.568	17.359	17.879	17.805	18.168
$\left(\frac{^{207}Pb}{^{204}Pb}\right)_M$	15.596	15.520	15.462	15.527	15.547	15.515	15.469	15.508	15.494	15.455	15.603	15.544	15.530
$\left(\frac{^{207}Pb}{^{204}Pb}\right)_I$	15.530	15.491	15.451	15.466	15.496	15.487	15.431	15.492	15.479	15.415	15.537	15.487	15.492
$\left(\frac{^{208}Pb}{^{204}Pb}\right)_M$	38.384	38.731	37.911	38.944	38.808	38.370	38.227	38.202	38.031	38.081	38.481	38.462	38.185
$\left(\frac{^{208}Pb}{^{204}Pb}\right)_I$	37.220	37.874	37.629	37.396	37.586	37.681	37.330	37.794	37.662	37.293	37.669	37.469	37.584
$\left(\frac{^{87}Sr}{^{86}Sr}\right)_M$	0.70640	0.70714	0.70724	0.70651	0.70722	0.70571	0.70859	0.70865	0.70667	0.70841	0.70684	0.70736	0.70710
$\left(\frac{^{87}Sr}{^{86}Sr}\right)_I$	0.70607	0.70640	0.70678	0.70590	0.70639	0.70546	0.70725	0.70710	0.70609	0.70757	0.70587	0.70650	0.70575

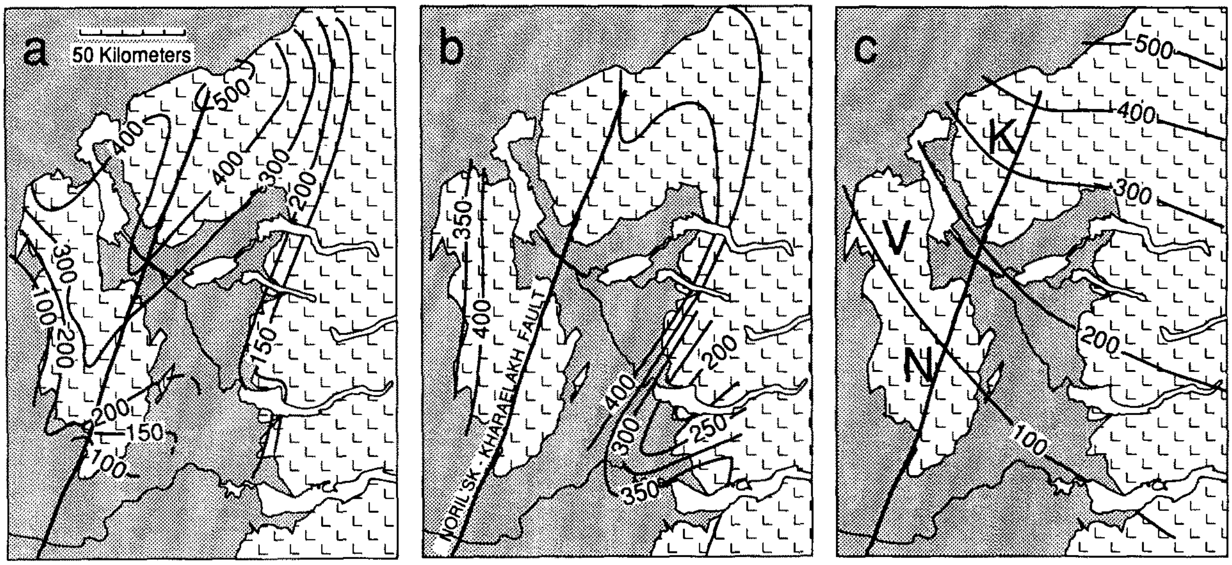

FIG. 3. Paleoisopach maps for the three lava assemblages in the Noril'sk area (FEDORENKO, 1979, 1991): (a) Ivakinsky-Gudchikhinsky; (b) Khakanchansky-Nadezhdinsky; and (c) Morongovsky-Samoedsky. Limits of basalt outcrop slightly generalized from Fig. 1. Only the upper Morongovsky lavas were contoured for panel (c) because younger lavas are strongly eroded. The Kharaelakh (K), Noril'sk (N), and Vologochan (V) depressions are indicated in (c). Contours in meters.

are discussed in detail by BAEDECKER (1987), and typical results from replicate analyses of standard rocks are presented by BACON and DRUITT (1988). In this report, we have recalculated all major- and trace-element data to anhydrous compositions, based on summation of the ten major oxides to 100%, following the assumption of total Fe as FeO.

Lead and strontium isotopic compositions were measured on a Finnigan-MAT 262 mass spectrometer in static mode at the USGS laboratory in Menlo Park, CA. Sample preparation for lead isotopic and concentration analyses followed the procedures of WOODEN et al. (1992). For strontium isotopic analyses, the HBr wash from the lead isotopic separation was collected, dried, dissolved in 2 N HNO_3, dried, and redissolved in 2 N HCl. Strontium was then separated, using 2 N HCl on a cation-exchange column and run on single Ta filaments. Within-run precision is ± 0.00002 or better. $^{87}Sr/^{86}Sr$ ratios are normalized to $^{88}Sr/^{86}Sr = 8.3752$. Standard NBS-987 gave an average $^{87}Sr/^{86}Sr$ ratio of 0.71026 ± 3 during the period of these analyses. For lead isotopic measurements, uncertainties in the ratios in individual runs are typically $\pm 0.05\%$ (2σ). Thermal-fractionation corrections are empirically determined from numerous measurements on standards NBS-981 and NBS-982, and average 0.11%/mass unit. Total uncertainties in isotopic ratios, which are dominated by variations in the thermal-fractionation correction, are estimated conservatively to be ± 0.08, 0.10, and 0.14% (2σ), respectively, for $^{206}Pb/^{204}Pb$, $^{207}Pb/^{204}Pb$, and $^{208}Pb/^{204}Pb$ ratios, on the basis of numerous runs on rock and metal standards over several years. To monitor the entire analytical scheme, standard whole-rock samples BCR-1 and BHVO-1 are processed periodically for lead and strontium isotopic analyses by the same techniques. During this study, measured (uncorrected for fractionation) lead isotopic ratios for fourteen samples of BHVO-1 ranged from 18.622–18.646 ($^{206}Pb/^{204}Pb$), 15.497–15.515 ($^{207}Pb/^{204}Pb$), and 38.104–38.160 ($^{208}Pb/^{204}Pb$), consistent with the fractionation correction factors determined from lead standards NBS-981 and NBS-982.

Isotopic data for the basalts are corrected for an age of 250 Ma (DALRYMPLE et al., 1991). Correction of the lead isotopic data uses measured lead (0.61–14.26 ppm), thorium (0.53–7.20 ppm), and uranium (0.12–3.24 ppm) contents, and uncertainties in the age-corrected data are greater than those associated with the measured data because of the additional uncertainties in the lead, thorium, and uranium contents. Generous analytical uncertainties of ± 3 percent for lead, ± 5 percent for thorium, and ± 10 percent for uranium produce significant errors only in the age-corrected $^{206}Pb/^{204}Pb$ ratios of the samples with the highest U/Pb ratios. Absolute uncertainties in the age-corrected $^{206}Pb/^{204}Pb$ ratios are generally less than 0.05 unit but may reach 0.10 unit for a few samples. These uncertainties in the age-correction calculations, however, are much less than the large lead isotopic variations that characterize the basalts (measured $^{206}Pb/^{204}Pb$ ratios range from 17.45 to 19.17; Table 1).

Neodymium isotopic compositions were measured on a Finnigan-MAT 262 mass spectrometer at Géosciences Rennes. Chemical techniques are slightly modified from WHITE and PATCHETT (1984). Neodymium isotopic analyses were made in a static mode, $^{143}Nd/^{144}Nd$ ratios were normalized to $^{146}Nd/^{144}Nd = 0.7219$, and the procedure gave a $^{143}Nd/^{144}Nd$ ratio of 0.511823 ± 12 (2σ) for the La Jolla neodymium standard.

MAJOR-ELEMENT, TRACE-ELEMENT, AND ISOTOPIC CHARACTERISTICS OF THE LAVA SUITES

Analytical data are listed in Tables 1 and 2 and selectively plotted in Figs. 4 through 12. When describing the chemistry of these rocks, our selection of elements has sometimes been based on (1) better analytical data for our data set (e.g., Ta in preference to Nb) or (2) availability of comparable data (e.g., as a measure of HREE depletion, we use $(Sm/Yb)_N$ rather than $(Gd/Yb)_N$ because gadolinium data are absent in many data sets). (The subscript "N" indicates that the elemental concentrations have been normalized using the primitive-mantle normalization values of HOFMANN, 1988.) In discussing trace-element ratios, the least compatible element during mantle magmatic processes is taken as the numerator (e.g., Rb/Sr, La/Sm, or Th/Ta). These ratios normally increase during fractionation or with decreasing percentage of partial melting. Measured and initial isotopic ratios and values are reported in Tables 1 and 2, but all discussion in this report is in terms of initial lead and strontium isotopic ratios and ϵ_{Nd} values.

The elements barium, cesium, potassium, and rubidium show considerable scatter in mantle-normalized element diagrams (Fig. 5). This group of elements is known to be mobile

Table 2. Isotopic compositions of Nd in selected samples

Sample	Suite	$^{147}Sm/^{144}Nd^*$	$(^{143}Nd/^{144}Nd)_M$	$(^{143}Nd/^{144}Nd)_I$	$\varepsilon_{Nd}(250\ Ma)$
16F-19	Sm_3	0.171	0.512618±8	0.512338	+0.4
SG-32-87	Hr_4	0.165	0.512681±6	0.512411	+1.9
SG-32-670	Hr_1	0.185	0.512691±6	0.512388	+1.4
SG-32-1255	Mk_1	0.171	0.512612±5	0.512332	+0.3
SG-32-1311	Mr_2	0.179	0.512688±6	0.512396	+1.6
SG-32-1645	Mr_1	0.150	0.512460±6	0.512214	-2.0
SG-32-1701	Nd_3	0.142	0.512408±8	0.512176	-2.7
SG-32-1838	Nd_2	0.146	0.512125±6	0.511887	-8.4
SG-32-2069	Nd_1	0.133	0.512062±5	0.511844	-9.2
SG-32-2144.3	Nd_1	0.136	0.512063±6	0.511841	-9.3
SG-32-2212.5	Nd_1	0.132	0.511967±5	0.511751	-11.0
1F-32	Tk	0.171	0.512458±9	0.512178	-2.7
1F-30	Tk	0.161	0.512422±6	0.512158	-3.1
1F-22	Tk	0.174	0.512605±8	0.512320	+0.1
SG-32-2245.5	Gd_2	0.161	0.512795±8	0.512531	+4.2
SG-32-2328	Gd_2	0.174	0.512773±5	0.512489	+3.4
SG-32-2357.5	Gd_1	0.162	0.512681±5	0.512415	+1.9
SG-32-2464.8	Sv	0.130	0.512371±4	0.512158	-3.1
SG-32-2533.7	Iv_3	0.116	0.512332±6	0.512142	-3.4
SG-32-2624.6	Iv_1	0.119	0.512501±4	0.512306	-0.2

*Calculated using Sm and Nd contents from Table 1.
$^{143}Nd/^{144}Nd$ normalized to $^{146}Nd/^{144}Nd = 0.7219$.
Estimated overall error, ± 0.000020.
Measured value for La Jolla standard, 0.511834±8 (2s).

during low-grade alteration, and their aberrant behavior, in addition to the petrographic evidence of alteration and the relatively high H_2O and occasionally high CO_2 contents measured in many samples, reflects the alteration undergone by these rocks. High strontium contents are measured in some samples (e.g., sample SG-32-2375.2 of picritic Gudchikhinsky basalt contains 900 ppm Sr). However, calculated initial $^{87}Sr/^{86}Sr$ [$(^{87}Sr/^{86}Sr)_I$] ratios vary systematically with respect to stratigraphic position (Fig. 6a), and there is generally a good correlation between $(^{87}Sr/^{86}Sr)_I$ ratios and initial ϵ_{Nd} ($\epsilon_{Nd,T}$) values ("T" taken as 250 Ma). Although interpretation of the strontium isotopic data for individual samples may be open to question, the overall trends are interpreted to reflect those of the lavas at the time of their eruption. The REE contents show coherent patterns in mantle-normalized element diagrams, with no obvious anomalies (Fig. 5). The neodymium isotopic data are least likely to have been affected by alteration.

In most respects, the major- and trace-element characteristics discussed in the following text are comparable to those reported by LIGHTFOOT et al. (1990b, 1993a,b) for a comparable, but more stratigraphically limited, suite of samples from the Noril'sk area.

Ivakinsky and Syverminsky

The two lowermost suites, the Ivakinsky and Syverminsky, comprise alkaline and subalkaline basalts with high contents of Na_2O, K_2O, and most incompatible trace elements (Fig. 5a), and varying SiO_2 contents (Fig. 4c). The three subsuites of the lowermost, Ivakinsky suite are alkaline and subalkaline basalts with overlapping Mg# but distinctive SiO_2 contents: Iv_1, 47.1–47.8; Iv_2, 51.1–52.2; and Iv_3, 53.6–53.8 wt% (Figs. 4a,c). The Mg# for the Syverminsky samples are distinctly higher than those for the Ivakinsky samples and are comparable to those of third-assemblage basalts (Fig. 4a); however, the REE characteristics of the Syverminsky suite are quite different from those of third-assemblage rocks. For both the Ivakinsky and Syverminsky suites, mantle-normalized element diagrams show a steep slope defined by REEs and thorium, with a maximum at barium and a sharp decrease for rubidium and cesium (Fig. 5a). There are negative tantalum anomalies in all samples (Fig. 4g); the smallest anomalies [$(Ta/La)_N \sim 0.8$] are seen for alkali trachybasalts of the Iv_1 subsuite (~47 wt% SiO_2), and larger anomalies [$(Ta/La)_N \sim 0.5$] characterize basalts of the Iv_2 and Iv_3 subsuites. The negative tantalum anomaly increases regularly with stratigraphic height for the three samples of the Syverminsky suite.

Isotopic variations in the Ivakinsky suite are related to composition and stratigraphic position (Figs. 6a,c, 7c, 8, 9b). The relatively silica-poor flows of the Iv_1 subsuite have the lowest $(^{87}Sr/^{86}Sr)_I$ ratios (0.7058–0.7065), the least negative $\epsilon_{Nd,T}$ value (−0.2), and the highest initial $^{206}Pb/^{204}Pb$ [$(^{206}Pb/^{204}Pb)_I$] ratios (17.8–18.2). The alkaline, more silica-rich basalts of the Iv_2 and Iv_3 subsuites have $(^{87}Sr/^{86}Sr)_I$ ratios = 0.7061–0.7076 and $(^{206}Pb/^{204}Pb)_I$ ratios = 17.4–17.7; a single analysed sample has $\epsilon_{Nd,T} = -3.4$. Basalts of the Syverminsky suite have isotopic compositions that continue the pattern of the Iv_2 and Iv_3 subsuites. The $(^{206}Pb/^{204}Pb)_I$ ratios are low (17.5–17.7), and $\epsilon_{Nd,T} = -3.1$ for the single analyzed sample. The $(^{87}Sr/^{86}Sr)_I$ ratios, however, range from 0.7055–0.7064 and thus are comparable to those of the Iv_1 subsuite; they increase with increasing MgO content.

Gudchikhinsky

Gudchikhinsky-suite lavas range from basalt to picrite (6.6–18.2 wt% MgO for the samples of Table 1, and 5–22 wt% MgO if other data sets are included, e.g., FEDORENKO, 1981; LIGHTFOOT et al., 1990b, 1993a,b). The Gd_1 subsuite is composed of a glomeroporphyritic flow, overlain by porphyritic basalts. Both samples of Gd_1 basalt from borehole SG-32 appear to be albitized, in comparison with the fresher samples analyzed by LIGHTFOOT et al. (1990b, 1993a,b), whose data show that the Gd_1 glomeroporphyritic basalt differs from the Syverminsky basalts in having lower REE contents, particularly LREEs. The Gd_1 porphyritic basalts are geochemically quite similar to the Syverminsky basalts, as stated by FEDORENKO (1981) on the basis of an extensive set of major-element data. Picritic and picrite-like basalts that form the Gd_2 subsuite are as much as 150–200 m thick; in restricted areas, picritic basalts interfinger with basalts of the Gd_1 subsuite. The Gd_2 picritic basalts of Table 1 contain 13.2–18.2 wt% MgO, but some samples contain as much as 22 wt% MgO (anhydrous). Average-weighted MgO contents for the Gd_2 subsuite range from 9–14.7 wt% in different parts of the Noril'sk area (NALDRETT et al., 1992, Fig. 5e), largely as a function of modal olivine content. Using Mg-Fe distribution, only the least magnesium rich of these picrites can be calculated to have been in equilibrium with Fo_{80} olivine (the most magnesian olivine reported in the Siberian basalts by RYABOV et al., 1985). Thus, whereas it is permissive that magmatic liquids containing 18 wt% MgO were erupted, we conclude that these picrites contained varying amounts of intratelluric olivine upon emplacement, much of which was entrained from an intermediate reservoir. Moreover, although the basalts of the suite have major-element compositions consistent with derivation by fractional crystallization of pa-

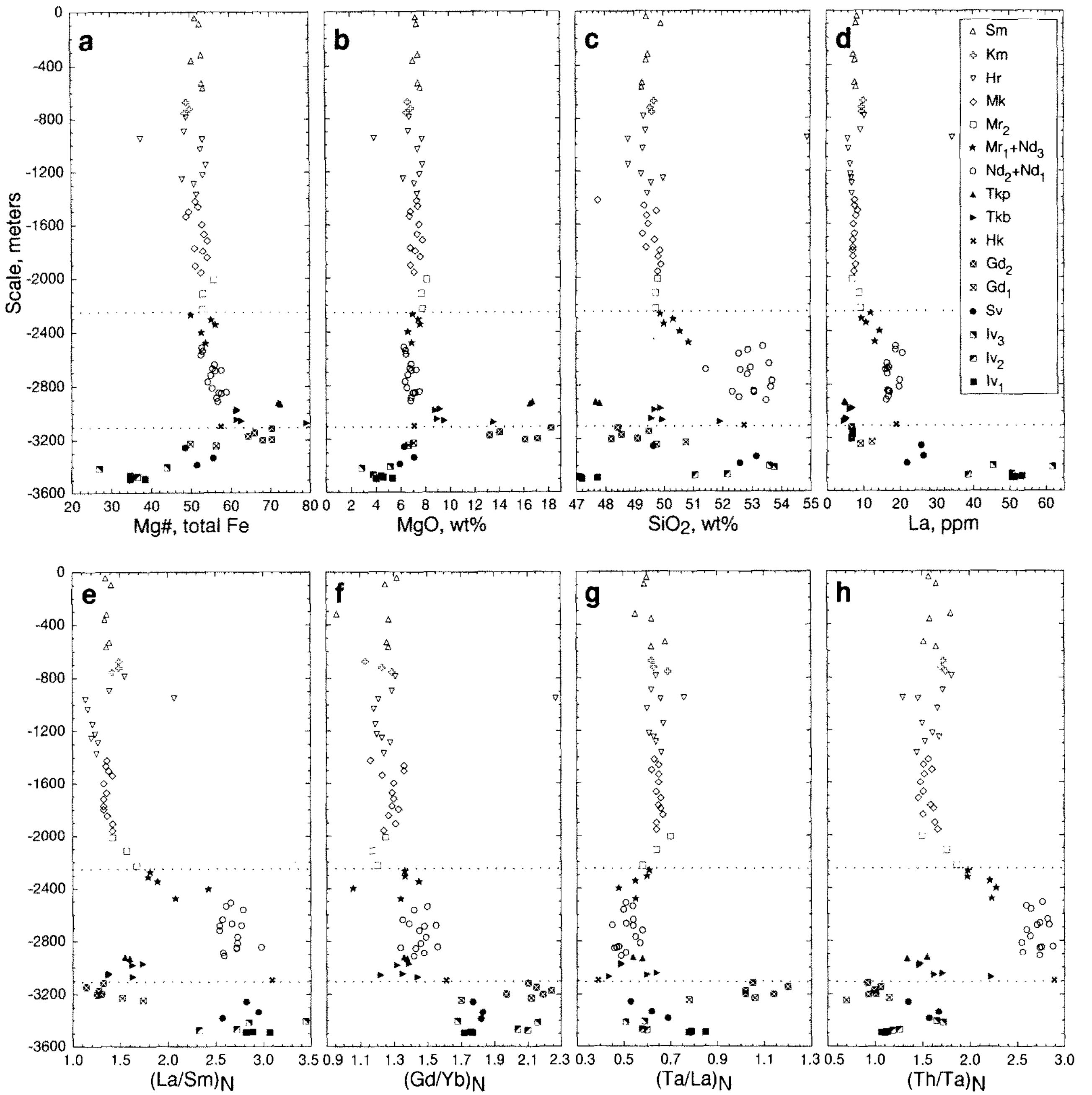

FIG. 4. Stratigraphic profiles of major- and trace-element chemistry throughout the basalt sequence for (a) Mg#, based on total Fe content; (b) MgO content; (c) SiO_2 content; (d) La content; (e) $(La/Sm)_N$ ratio; (f) $(Gd/Yb)_N$ ratio; (g) $(Ta/La)_N$ ratio; and (h) $(Th/Ta)_N$ ratio. Primitive-mantle-normalization values from HOFMANN (1988). Dotted lines aid in distinguishing the stratigraphic progression through the first, second, and third basalt assemblages.

rental picritic liquids, such ratios as $(La/Sm)_N$ and $(Ta/Yb)_N$ change significantly within the suite and rule out a simple crystallization relation, as do their isotopic compositions. General characteristics of the rocks are moderate contents of incompatible elements (for a given Mg#) and moderate $(La/Sm)_N$ but relatively high $(Gd/Yb)_N$ ratios (Fig. 4e, f). With near-chondritic $(Ta/La)_N$ ratios (Fig. 4g), the absence of a negative tantalum anomaly distinguishes rocks of the Gudchikhinsky suite from those of all other Siberian basalt suites.

The Gd_1 subsuite of marginally alkaline basalts can be distinguished isotopically from the picritic Gd_2 subsuite by its lower $\epsilon_{Nd,T}$ value (+1.9 vs. +3.4 and +4.2; Fig. 8) and lower $(^{207}Pb/^{204}Pb)_I$ ratios (15.45–15.49 vs. 15.53–15.57; Fig. 7a); $(^{87}Sr/^{86}Sr)_I$ ratios broadly overlap (0.7064–0.7067 vs. 0.7057–0.7067; Fig. 6). Picrites of the Gudchikhinsky suite are characterized by uniformly high $(^{207}Pb/^{204}Pb)_I$ ratios (Fig. 7a), and the entire suite has high $(^{87}Sr/^{86}Sr)_I$ ratios relative to $\epsilon_{Nd,T}$ values (Fig. 8a). Although it is presently uncertain whether these isotopic characteristics are magmatic or are related to postcrystallization alteration, coherency in the isotopic data has led us to accept the measured data as meaningful.

Tuklonsky

The Kakanchansky suite, which consists predominately of basaltic tuffs, is represented by a single sample of basaltic tuff (SG-32-2226.7, Table 1). In the eastern part of the Noril'sk area, minor flows occur within the Kakanchansky suite that are similar to the Tuklonsky basalts, and in the western part of the area there occur flows similar to those of the Nd_1 subsuite. The Tuklonsky basalts and picrites of the second assemblage show a wide range in major-element contents (e.g., 8.8–16.7 wt% MgO) but show little variation in trace-element ratios. We might attempt to explain the picrite-basalt association in this suite by fractional crystallization, but the neodymium, strontium, and lead isotopic data indicate a more complex relation. The Tuklonsky picrites vary in stratigraphic position and have a relatively small volume (flows less than 35 m thick and a few kilometers long). The volume of the Tuklonsky picrites in the Noril'sk area has been estimated at 180 km^3, in comparison with 14,860 km^3 for the Gudchikhinsky picrites (FEDORENKO, 1981). The Tuklonsky picrites probably also carried intratelluric olivine (Fo_{80} by electron microprobe) from an intermediate reservoir and thus do not represent eruption of high-Mg liquids.

The overall trace-element characteristics of the Tuklonsky picrites differ significantly from those of Gudchikhinsky picrites. The Tuklonsky picrites contain slightly lower contents of incompatible elements and TiO_2, FeO, nickel, and chromium, but higher Al_2O_3 and strontium contents at a given Mg#. Their chondrite-normalized REE patterns are notably flatter; the extent of enrichment in LREEs is similar in the Gudchikhinsky and Tuklonsky picrites (Fig. 4e), but the conspicuous depletion of HREEs that characterizes the Gudchikhinsky picrites is absent in the Tuklonsky picrites (Fig. 4f). Basalts and picrites of the Tuklonsky suite have relatively large, negative tantalum anomalies (Fig. 4g).

The Tuklonsky picrites are distinctive from the Tuklonsky tholeiites and all other lava suites because of their very low $(^{206}Pb/^{204}Pb)_I$ ratios (16.8–17.0 vs. 17.3–17.9 for the tholeiites; Fig. 7). With respect to other samples of the Noril'sk lava sequence analyzed in this study, the Tuklonsky picrites have slightly retarded $(^{87}Sr/^{86}Sr)_I$ ratios (0.7056 ± 1) for their $\epsilon_{Nd,T}$ values (−2.7 and −3.1; Fig. 8). In contrast, the single tholeiitic basalt sample analyzed for strontium and neodymium isotopic composition is on the main $(^{87}Sr/^{86}Sr)_I$ vs. $\epsilon_{Nd,T}$ trend for Noril'sk [$(^{87}Sr/^{86}Sr)_I = 0.7053$ and $\epsilon_{Nd,T} = 0.1$]. The other two tholeiitic basalt samples were analyzed only for strontium isotopic composition and have higher $(^{87}Sr/^{86}Sr)_I$ ratios (0.7059 and 0.7060). For the three basalt samples from locality 1F, $(^{87}Sr/^{86}Sr)_I$ ratios increase with increasing stratigraphic position (Fig. 6a) and negatively correlate with $(^{206}Pb/^{204}Pb)_I$ ratios (Fig. 9a). These isotopic data indicate that the Tuklonsky picrites and tholeiites are not simply related by olivine addition or subtraction.

Nd_1 and Nd_2

All the Nadezhdinsky basalts are strongly enriched in LREEs but have relatively flat HREE patterns (Fig. 4e, f); they have the highest $(Th/Ta)_N$ ratios found in any SFBP basalt suite. Basalts of the Nd_1 and Nd_2 subsuites have low MgO contents (6.3–7.3 wt%) but moderate Mg# that decrease irregularly with increasing stratigraphic height (from ~0.57–~0.53), and SiO_2 contents that range from 51.4–53.7 wt% (Fig. 4a,b,c). Among SFBP basalts, those of the Nd_1 and Nd_2 subsuites are notably depleted in copper, nickel, and PGEs; yet the transition from Nd_1 to Nd_2 is marked by a sharp increase in contents of copper (10–75 ppm), nickel (24–53 ppm), and chromium (72–106 ppm). This marked change in transition-metal contents at the Nd_1-Nd_2 boundary is not evidenced in the large-ion-lithophile (LIL)-element or isotopic data (Figs. 4d, 6a,c) and so is interpreted as due largely to a change in the efficiency of sulfide-melt extraction (NALDRETT et al., 1992; BRÜGMANN et al., 1993).

Basalts of the Nd_1 and Nd_2 subsuites have uniformly high $(^{87}Sr/^{86}Sr)_I$ ratios (0.7074–0.7087) and correspondingly low $\epsilon_{Nd,T}$ values (−8.4 to −11). Three of the four samples analyzed anchor the bottom of the $(^{87}Sr/^{86}Sr)_I$ vs. $\epsilon_{Nd,T}$ trend for the Noril'sk lava sequence; the fourth, the stratigraphically lowest Nd_1 sample, lies to the left of this trend (Fig. 8). $(^{87}Sr/^{86}Sr)_I$ ratios increase irregularly from the lowest sampled Nd_1 flow to the uppermost Nd_1 and lowermost Nd_2 flows, followed by a decline in $(^{87}Sr/^{86}Sr)_I$ ratios (Fig. 6a; better revealed by data of LIGHTFOOT et al., 1993a). Samples of the Nd_1 and Nd_2 subsuites have relatively low $(^{206}Pb/^{204}Pb)_I$ ratios (17.3–17.8), a feature that characterizes most of the SiO_2-rich samples in the Noril'sk lava sequence (Fig. 7; see the Iv_2, Iv_3, and Syverminsky discussions in the preceding text). In addition, these samples define a clear linear trend, parallel to, but above, the STACEY and KRAMERS (1975) model growth curve for average crust on the $(^{206}Pb/^{204}Pb)_I$ vs. $(^{208}Pb/^{204}Pb)_I$ diagram (Fig. 7b), and lie in the lead isotopic field defined by the relatively SiO_2-rich basalts of the Noril'sk lava sequence (Fig. 7).

Nd_3 and Mr_1

Basalts of the Nd_3 and Mr_1 subsuites have chemical features transitional between those of the Nd_1 and Nd_2 subsuites and those of all the overlying basalts. This transitional, but seemingly coherent, group of rocks includes both glomeroporphyritic (Nd_3) and aphyric (Mr_1) basalts. With increasing stratigraphic height, there is a progressive decrease in SiO_2 content and $(La/Sm)_N$, and an increase in $(Ta/La)_N$ and $\epsilon_{Nd,T}$ values (Figs. 4, 8).

The isotopic systematics of the Nd_3 subsuite show a sharp change from those of the two lower subsuites but are quite similar to those of the single sample analyzed from the lower Morongovsky (Mr_1) subsuite. The isotopic compositions of Nd_3 and Mr_1 samples ($(^{87}Sr/^{86}Sr)_I$ = 0.7062–0.7064, $\epsilon_{Nd,T}$ = −2.0 to −2.7, and $(^{206}Pb/^{204}Pb)_I$ = 17.8–18.0) clearly are intermediate to those obtained for samples from the Nd_1-Nd_2 and upper Morongovsky (Mr_2) subsuites and all other stratigraphically higher basalt suites on plots of elemental contents vs. isotopic ratios, or isotopic ratios vs. stratigraphic height; in each plot the data generally lie along a linear trend (Figs. 6a, 7, 8, 9). Simple physical mixing of magmas from these two endmember groups is an acceptable, though not necessarily exclusive, process to produce the isotopic and compositional characteristics of the Nd_3 and Mr_1 subsuites.

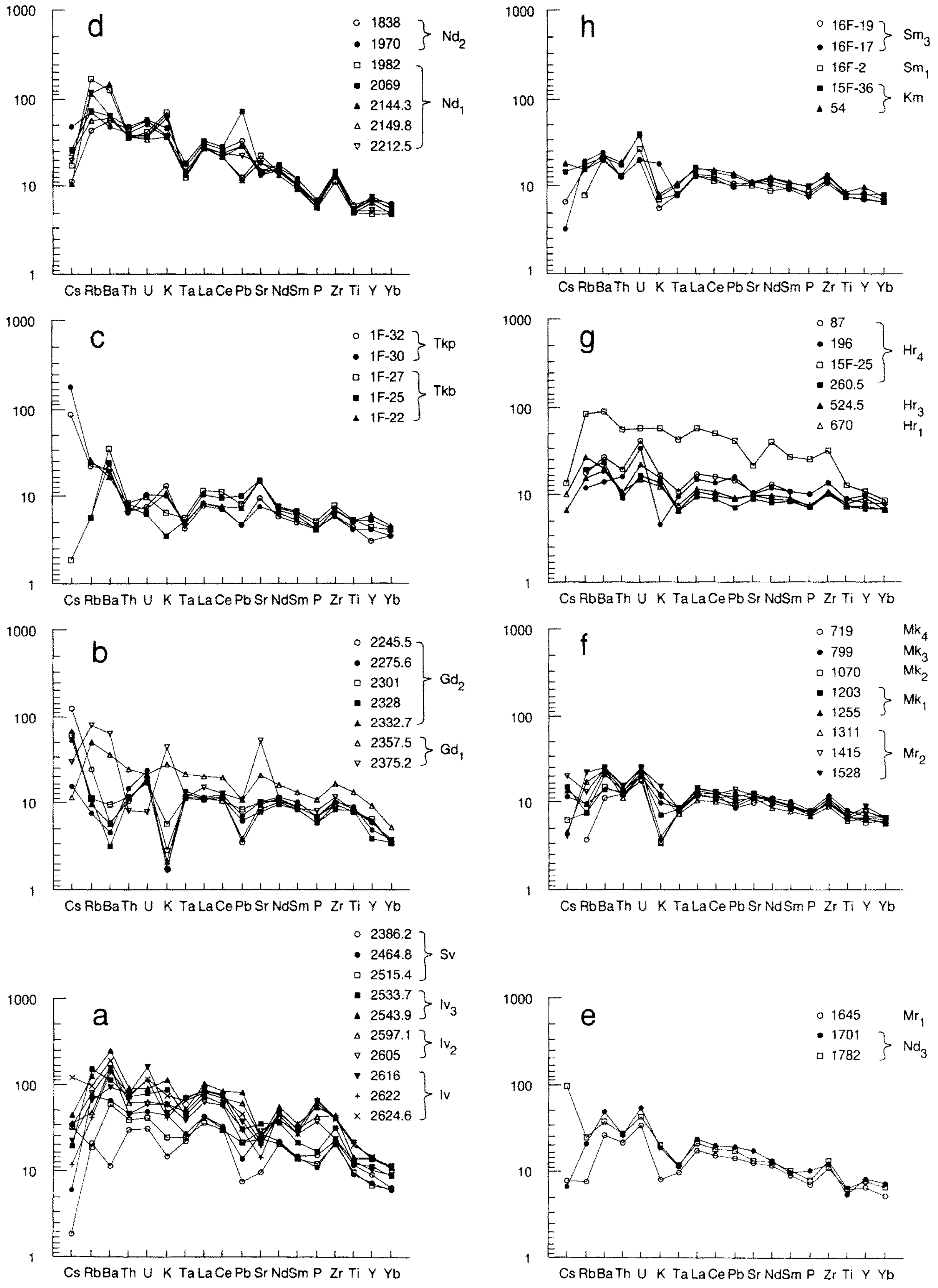
d
1838
1970
Nd2
1982
2069
2144.3
2149.8
2212.5
Nd1
h
16F-19
16F-17
Sm3
16F-2
Sm1
15F-36
54
Km
c
1F-32
1F-30
Tkp
1F-27
1F-25
1F-22
Tkb
g
87
196
15F-25
260.5
Hr4
524.5
Hr3
670
Hr1
b
2245.5
2275.6
2301
2328
2332.7
Gd2
2357.5
2375.2
Gd1
f
719
Mk4
799
Mk3
1070
Mk2
1203
1255
Mk1
1311
1415
1528
Mr2
a
2386.2
2464.8
2515.4
Sv
2533.7
2543.9
Iv3
2597.1
2605
Iv2
2616
2622
2624.6
Iv
e
1645
Mr1
1701
1782
Nd3
1000
100
10
1
Cs Rb Ba Th U K Ta La Ce Pb Sr Nd Sm P Zr Ti Y Yb

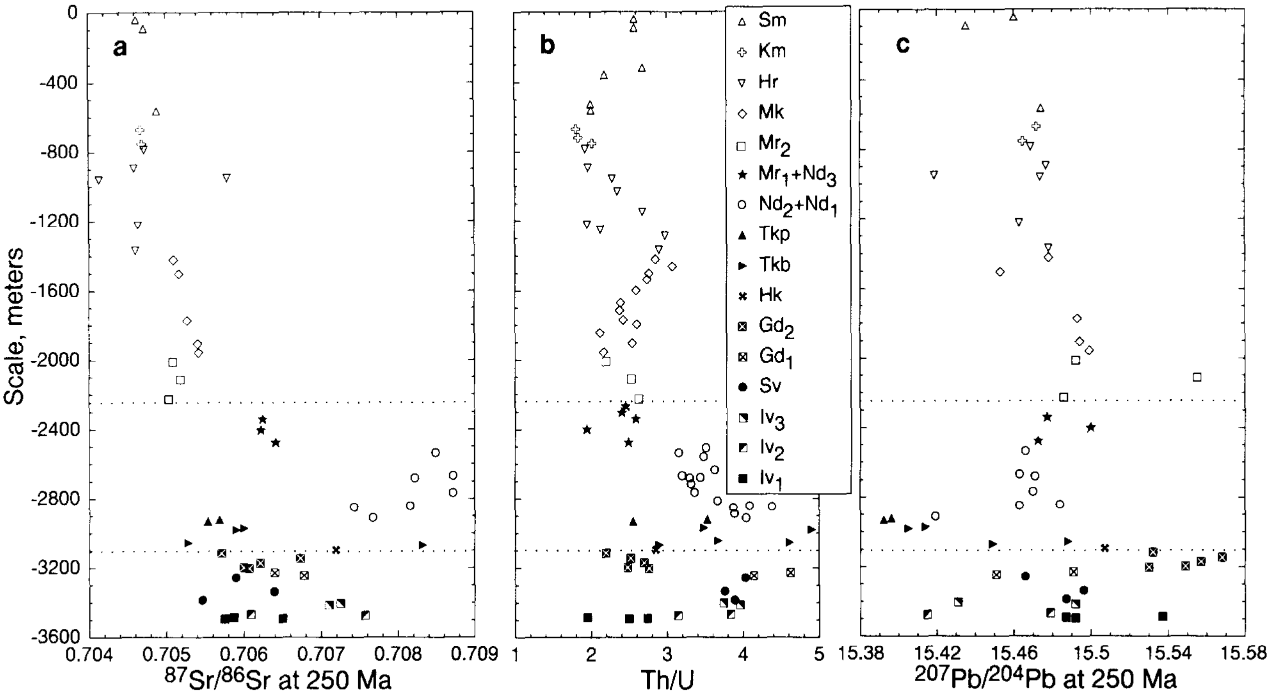

FIG. 6. Stratigraphic profiles through the basalt sequence for (a) $(^{87}Sr/^{86}Sr)_I$ ratio; (b) Th/U ratio; and (c) $(^{207}Pb/^{204}Pb)_I$ ratio.

Upper Morongovsky (Mr_2) to Samoedsky

Above the Nd_3 and Mr_1 subsuites, five basalt suites constitute the third assemblage, which forms a 2,300-m-thick section that shows relatively little compositional variation. Almost all samples have MgO contents between 6.3 and 7.8 wt%, Mg# between 0.48 and 0.56, and SiO_2 contents between 47.8 and 49.9 wt%. An exception is sample 15F-25, from a single Ikonsky andesitic basalt flow, 10 m thick and 0.5 km long, in the Kharaelakhsky suite; it has chemical characteristics similar in many ways to Iv_2 and Iv_3 alkaline and subalkaline basalts (Figs. 4, 5). In the third-assemblage basalts, variations in trace-element abundances, trace-element ratios, and isotopic compositions are moderate; several ratios show systematic trends, with changes in these trends largely occurring within the Kharaelakhsky suite at the level where the Ikonsky flow occurs [e.g., lanthanum, thorium, and uranium contents and ratios involving REEs (Fig. 4) and Th/U (Fig. 6b)]. Basalts of the third assemblage are moderately enriched in LREEs and have relatively flat HREE patterns, quite similar to those of the Tuklonsky picrites (Fig. 4e, f). Tantatum anomalies, though ubiquitous, are smaller than in rocks of the second assemblage (Fig. 4g).

Isotopic variations in the Mr_2 subsuite and the four uppermost basalt suites are much more limited than those found in the earlier lava suites. With the exception of two samples, $(^{87}Sr/^{86}Sr)_I$ = 0.7046–0.7054, $\epsilon_{Nd,T}$ = 0.3–1.9, and $(^{206}Pb/^{204}Pb)_I$ = 17.6–18.2 (Figs. 6a, 7, 8, 9). The exceptions are in the Hr_4 subsuite: (1) sample SG-32-260.5 is a compositionally normal tholeiite with the lowest $(^{87}Sr/^{86}Sr)_I$ ratio (0.7041) determined in this study, and (2) sample 15F-25, the high-silica Ikonsky andesitic basalt, is compositionally and isotopically similar to the Iv_2, Iv_3, and Sverminsky basalts.

Whereas limited isotopic variation within these third-assemblage suites is their primary feature, systematic isotopic variations are found in some of the suites and provide important insights into the magmatic processes that produced the upper lava sequence. In a stratigraphic profile, the uniformly higher $(^{87}Sr/^{86}Sr)_I$ ratios of the Mokulaevsky samples and the regular decrease in $(^{87}Sr/^{86}Sr)_I$ ratios (0.7054–0.7051) upward in this suite are notable (Fig. 6a). Steps in the $(^{87}Sr/^{86}Sr)_I$ profile are found at the boundaries between the Morongovsky and Mokulaevsky suites (0.7051–0.7054) and between the Mokulaevsky and Kharaelakhsky suites (0.7051–0.7046). With the exceptions noted in the preceding text, variation in $(^{87}Sr/^{86}Sr)_I$ ratio in the three uppermost suites is quite small (0.7046–0.7049). Neodymium isotopic data

FIG. 5. Mantle-normalized element diagrams (WHEATLEY and ROCK, 1988) for the basalt suites (Table 1), normalized to HOFMANN's (1988) primitive-mantle values. Lettered in the order of superposition: (a) Ivakinsky (Iv) and Syverminsky (Sv); (b) Gudchikhinsky (Gd_1, basalts; Gd_2, picrites); (c) Tuklonsky (Tkb, basalts; Tkp, picrites); (d) Lower and Middle Nadezhdinsky (Nd_1 and Nd_2); (e) Upper Nadezhdinsky (Nd_3) and Lower Morongovsky (Mr_1); (f) Upper Morongovsky (Mr_2) and Mokulaevsky (Mk); (g) Kharaelakhsky (Hr); and (h) Kumginsky (Km) and Samoedsky (Sm). Leading "SG-32-" deleted for all borehole samples.

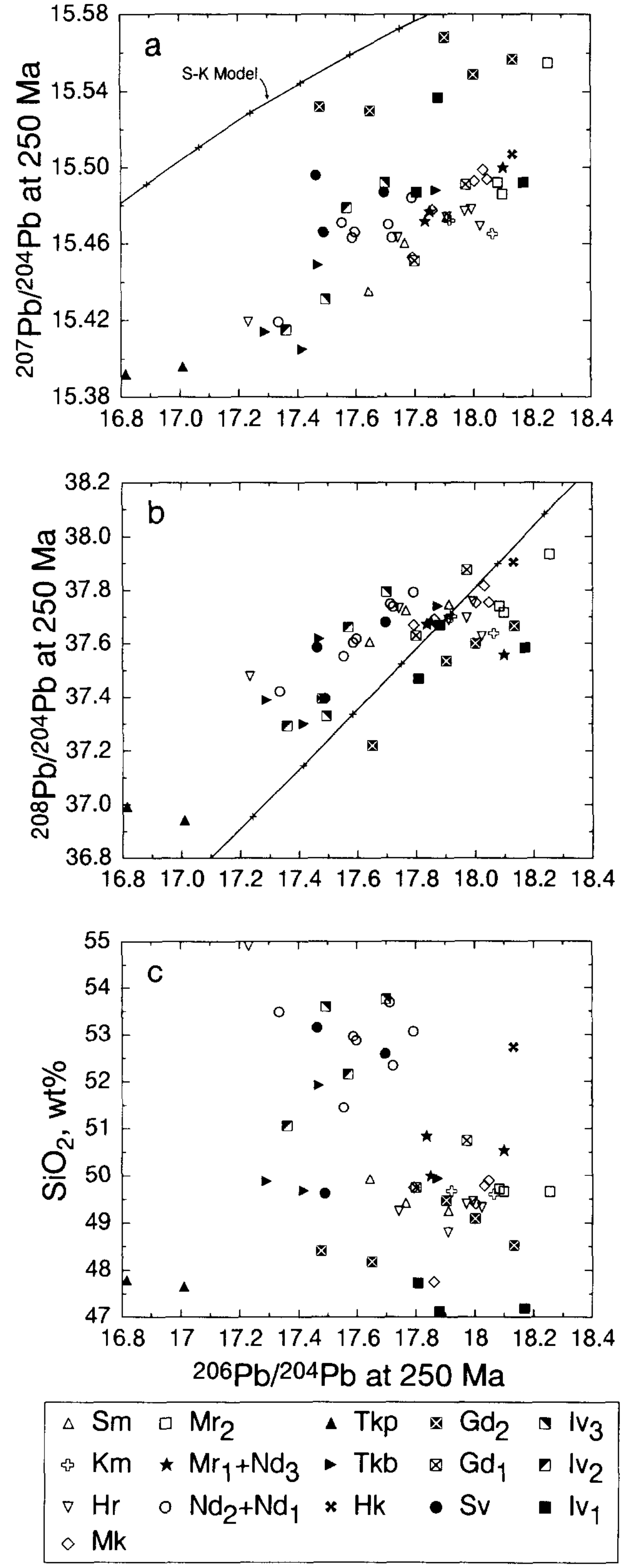

FIG. 7. (a) $(^{206}Pb/^{204}Pb)_I$ vs. $(^{207}Pb/^{204}Pb)_I$ ratios; (b) $(^{206}Pb/^{204}Pb)_I$ vs. $(^{208}Pb/^{204}Pb)_I$ ratios; and (c) $(^{206}Pb/^{204}Pb)_I$ ratio vs. SiO_2 content. All data corrected for 250 m.y. of radiogenic-lead growth, using measured lead, thorium, and uranium contents. STACEY and KRAMERS' (1975) model growth curves for average crust shown for reference.

for these five suites are limited; available data lie along the upper part of the main $(^{87}Sr/^{86}Sr)_I$ vs. $\epsilon_{Nd,T}$ correlation trend for the Noril'sk lava sequence (Fig. 8a). The lead isotopic systematics are clearly the most variable isotopic parameter for this group. Although the variation is somewhat random, limiting bounds of the data trends with respect to stratigraphic position indicate that $(^{206}Pb/^{204}Pb)_I$ and $(^{207}Pb/^{204}Pb)_I$ ratios decrease upward, whereas $(^{208}Pb/^{204}Pb)_I$ ratios are relatively constant (Figs. 6c, 7a,b). The Mokulaevsky suite shows a stratigraphically upward decrease in all lead isotopic ratios that roughly correlates with a decrease in $(^{87}Sr/^{86}Sr)_I$ ratios (Fig. 9a).

GEOCHEMICAL AND ISOTOPIC VARIATIONS WITHIN THE SFBP

The geochemical and isotopic data presented in the preceding text clearly indicate a varied and complex magmatic system. These data are explicable, however, within a framework based on (1) the three basalt assemblages originally

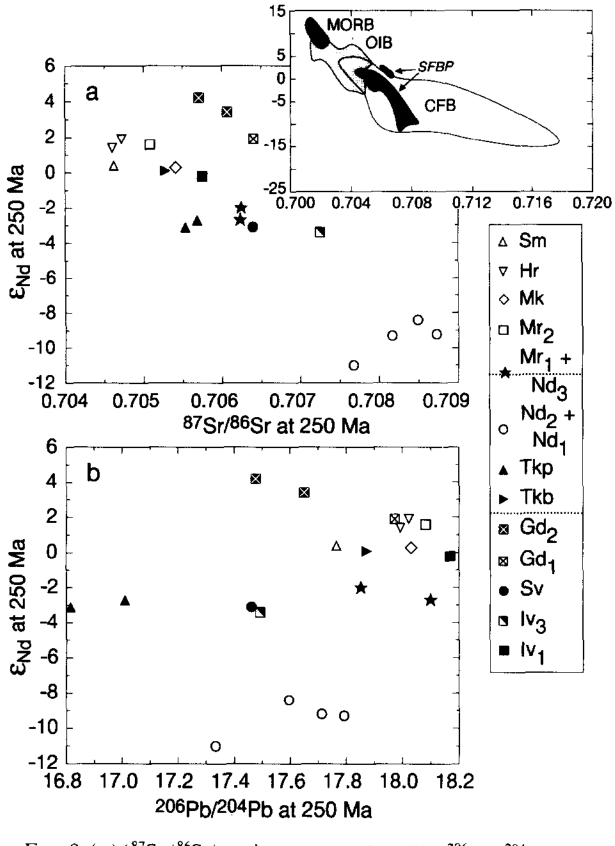

FIG. 8. (a) $(^{87}Sr/^{86}Sr)_I$ ratio vs. $\epsilon_{Nd,T}$ value; (b) $(^{206}Pb/^{204}Pb)_I$ ratio vs. $\epsilon_{Nd,T}$ value (data set of Table 2). Dotted lines in the legend separate the three basalt assemblages (see text). MORB, midoceanic-ridge basalt; OIB, oceanic-island basalt (HOFMANN et al., 1986; K. P. Jochum, unpubl data); CFB, continental flood basalt (CARLSON and HART, 1988; CARLSON, 1991; LIGHTFOOT and HAWKESWORTH, 1988; LIGHTFOOT et al., 1990a; MAHONEY, 1988). Data for inset presented for 250 Ma.

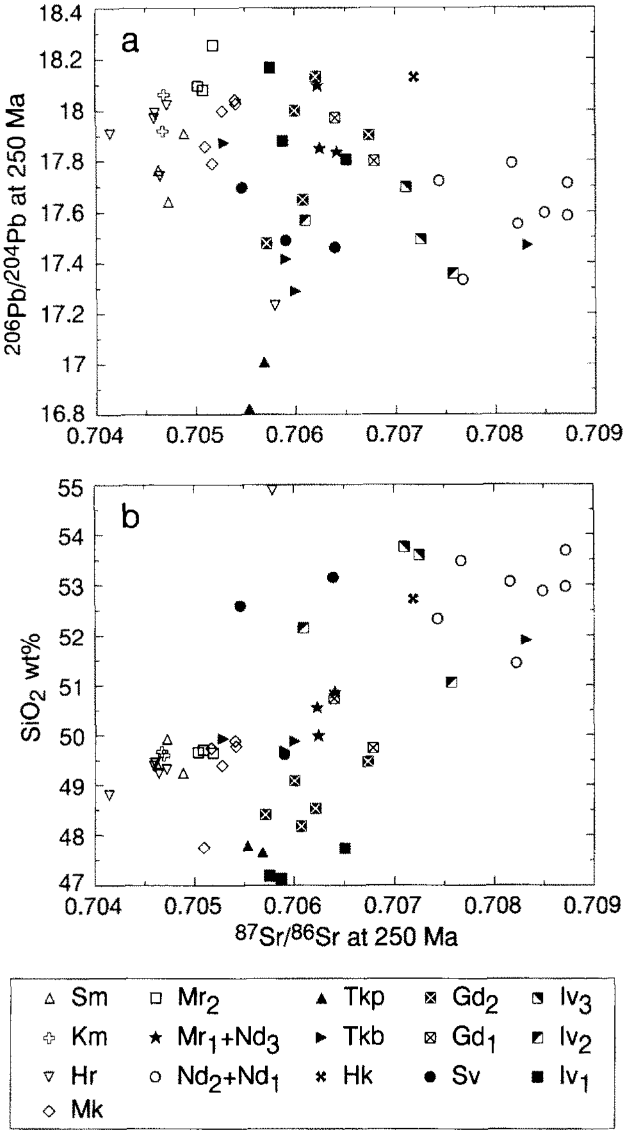

FIG. 9. (a) $(^{87}Sr/^{86}Sr)_I$ vs. $(^{206}Pb/^{204}Pb)_I$ ratios; (b) $(^{87}Sr/^{86}Sr)_I$ ratio vs. SiO_2 content.

proposed for the volcanic sequence on the basis of petrology, chemical composition, and paleotectonic reconstruction (FEDORENKO, 1981) and now substantiated by more extensive trace-element and isotopic data, and (2) several major controls on the geochemical and isotopic compositions of the individual volcanic suites. These controls are (a) differences in parental-magma geochemistry caused by variations in source geochemistry, in source mineralogy as a result of melting at different pressures and temperatures, and in the percentage of melting; (b) fractionation of parental magmas, varying amounts of assimilation/partial melting of crustal rocks during fractionation, and variation in the composition of the contaminants; and (c) mixing of magmas.

The Ivakinsky and Syverminsky suites of the first assemblage have high incompatible-element contents and high $(La/Sm)_N$ and $(Gd/Yb)_N$ or $(Sm/Yb)_N$ ratios (Figs. 4e,f, 11; LIGHTFOOT et al., 1990b, 1993a,b). Most of the lava flows in these suites are strongly fractionated, as indicated by low Mg# (Fig. 4a). These compositional characteristics find some parallels in the compositions of high-Ti CFBs, such as those from the Karoo or Parana basalt provinces (DUNCAN et al., 1984; PEATE et al., 1992), or in the compositions of ocean-island basalts (OIBs). They can be explained if a mantle source with near-chondritic $(Gd/Yb)_N$ ratios melted at relatively high pressure under conditions in which garnet was a residual phase; high contents of incompatible trace elements suggest that the percentage of melting in the mantle source region was relatively low. The tendency of the more silica-rich samples of these two suites to have high $(Th/Ta)_N$ ratios, relatively high $(^{87}Sr/^{86}Sr)_I$ ratios, and low $(^{206}Pb/^{204}Pb)_I$ ratios indicates that fractionation was accompanied by crustal contamination. The near-vertical trend of Syverminsky-suite samples on the plot of tantalum vs. thorium contents (Fig. 10) indicates that mixing occurred between batches of magma that had diverse fractionation/contamination histories. As discussed by LIGHTFOOT et al. (1993b) for a similar plot of zirconium versus thorium contents, fractionation and partial melting can cause variations in the contents of these strongly to moderately incompatible elements only along lines of nearly constant ratio. Contamination with crustal material, characterized by high thorium contents and high Th/Ta ratios, is needed to produce the Th/Ta ratios of about 4.5 in the lower Syverminsky flows; Th/Ta ratios near 2.3 in the upper Syverminsky flows reflect eruption of magma with a Th/Ta ratio near that of primitive mantle. The trend of the Syverminsky data suggests that magma with a composition comparable to that of the tholeiitic members of the overlying Gudchikhinsky suite was one of the mixing components. This mixing of early, crustally contaminated magma with less contaminated and distinct magma resembling an immediately overlying suite is repeated at least once again, as represented by the contrast between the compositions of the Nd_1-Nd_2 and Nd_3 basalts of the Nadezhdinsky suite.

The Gudchikhinsky suite has some perplexing aspects: it is characterized by high $(Gd/Yb)_N$ or $(Sm/Yb)_N$ ratios similar to those of the Ivakinsky and Syverminsky suites, but lower $(La/Sm)_N$ ratios comparable to those of thestratigraphically higher suites (Figs. 4e,f, 11a,b). The combination of high $(Gd/Yb)_N$ or $(Sm/Yb)_N$ ratios and high contents of incompatible elements also suggests the presence of residual garnet in its source and a relatively low percentage of melting. The geochemical characteristics of the Gudchikhinsky suite are transitional in many respects between those typical of the first assemblage and those of the upper two assemblages. Its $(Th/Ta)_N$ ratios are nearer to unity than those for any other suite and therefore most closely resemble those of asthenospheric mantle; however, it has the highest $(^{207}Pb/^{204}Pb)_I$ relative to $(^{206}Pb/^{204}Pb)_I$ ratios and unusually high $(^{87}Sr/^{86}Sr)_I$ ratios relative to $\epsilon_{Nd,T}$ values (Figs. 7, 8). These isotopic features might be related to postcrystallization alteration, but the REE characteristics and $(Th/Ta)_N$ ratios should not be affected by alteration and thus indicate a unique petrogenesis for this suite relative to others in the Noril'sk lava sequence. The range of $\epsilon_{Nd,T}$ values (−3 to +4, Fig. 8) in all first-assemblage lavas is similar to that of certain other CFBs where even larger ranges are observed (e.g., Deccan, MAHONEY, 1988; Columbia River, CARLSON, 1984) and coincides with the lower $\epsilon_{Nd,T}$ part of the OIB field. Our interpretation of this range of values is that the more negative $\epsilon_{Nd,T}$ values probably represent the effects of crustal contamination, as indicated by the $(^{87}Sr/^{86}Sr)_I$ ratios and compositional data. The modestly positive $\epsilon_{Nd,T}$ values that characterize the Gudchikhinsky suite are consistent with a model of partial melting of an OIB-like mantle source.

We have few data for the tuffaceous Kakanchansky suite that initiates the second assemblage. The second suite in this assemblage, the Tuklonsky, is more depleted in LIL elements than any other suite in the lava sequence (Figs. 4d, 12a). The relatively flat REE patterns and low REE contents that characterize this suite mark a major change to relatively high-percentage melting of mantle sources without garnet, presumably an indication of melting at lower pressures than those characteristic of first-assemblage magmas. The lowermost flow in the Tuklonsky suite has initial isotopic compositions similar to those found in third-assemblage basalts (Figs. 7, 8, 9). Overlying Tuklonsky flows have higher $(^{87}Sr/^{86}Sr)_I$ ratios and lower initial lead (Fig. 9a) and neodymium (LIGHTFOOT et al., 1993a) isotopic compositions. These isotopic trends seemingly are forerunners of similar but more extreme trends seen in the overlying Nadezhdinsky suite. LIGHTFOOT et al. (1993a,b) argue that the Nadezhdinsky suite represents Tuklonsky-like magmas modified by contamination with crustal material—a conclusion with which we agree. LIGHTFOOT et al. (1990b) had originally suggested that Mokulaevsky-like magmas were parental to the Nadezhdinsky suite, a model that required assimilation of as much as 40% of tonatitic upper crust. However, the geochemical characteristics of the Tuklonsky suite are such that much less contamination of a Tuklonsky-like parental magma would be required. The isotopic characteristics of the Tuklonsky suite, especially the combined lead and strontium isotopic data (Fig. 9a) that emphasize relatively unradiogenic lead isotopic compositions for the second assemblage, also favor a connection between the Tuklonsky and the Nd_1 and Nd_2 subsuites (it is important to continue to distinguish these two subsuites from the Nd_3 subsuite, as discussed in the following text). Samples of the Nd_1 and Nd_2 subsuites have thorium and tantalum contents quite different from those of most other lava suites (Fig. 10), and crustal contamination of Tuklonsky-like magmas is a reasonable way to produce the observed, relatively high Th/Ta ratios, as discussed for the Syverminsky suite. Most of the Nd_1 and Nd_2 samples, however, have relatively constant Th/Ta ratios over a range of thorium and tantalum contents, supporting the fact that fractionation was an important process within these subsuites, once contamination had established the new Th/Ta ratio.

The uppermost subsuite of the Nadezhdinsky, Nd_3, and the lowermost subsuite of the Morongovsky, Mr_1, mark the break between the second and third assemblages. Both the geochemical and isotopic characteristics of these subsuites are transitional between the Nd_1-Nd_2 and Mr_2 subsuites. The pattern of data on the plot of thorium vs. tantalum contents (Fig. 10) and on most other compositional and isotopic diagrams is most readily interpreted to result from magma mixing, produced by an influx of upper Morongovsky-like magma into a magmatic system previously dominated by Nd_1 and Nd_2 magmas. This stage of magma mixing ended second-assemblage magmatism, and very low LIL-element, Tuklonsky-like magmas are not observed again in the Noril'sk lava sequence (Fig. 12a). The change from second- to third-assemblage magmatism is associated with a notable shift in the principle locus of eruptive magmatic activity to the northeast (Fig. 3) and an increase in the volumes of magma erupted (Fig. 2).

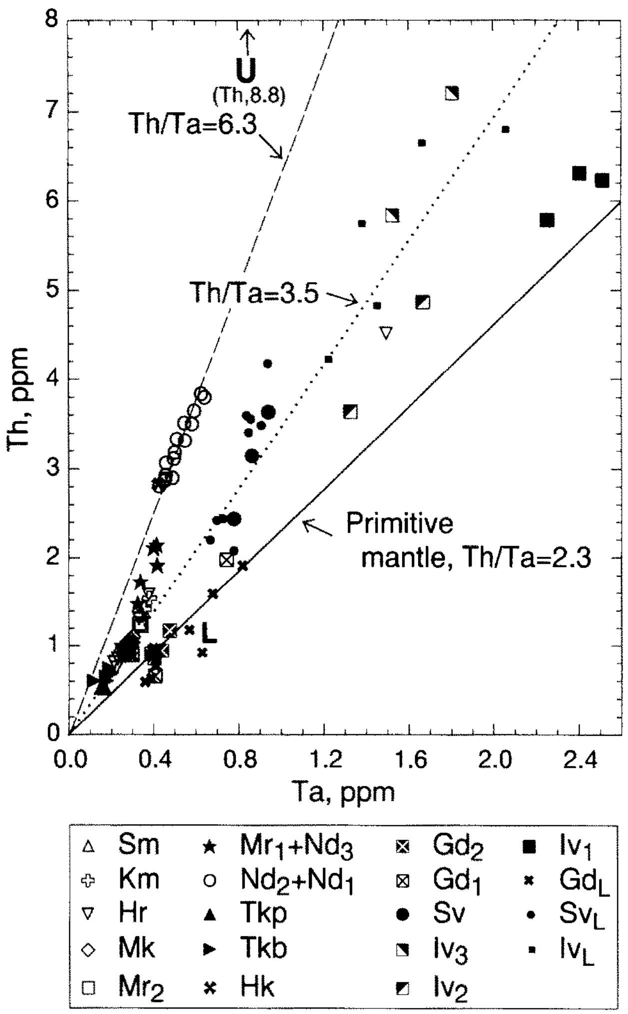

FIG. 10. Tantalum versus thorium contents. Large symbols represent our full seventy-nine sample data set; smaller dots, squares, and crosses represent data from LIGHTFOOT et al. (1990b, 1993a,b) for the designated basalt suites. Primitive-mantle ratio from HOFMANN (1988). L, lower continental crust, based on TAYLOR and MCLENNAN (1985). U, average upper continental crust (CONDIE, 1993).

Third-assemblage basalts are notable for their relatively constant major- and trace-element compositions and trace-element ratios; however, both isotopic compositions and some trace-element contents show significant variations within this assemblage. Trace-element variations are most notable in ratios involving U; Th/U ratios show significant changes at

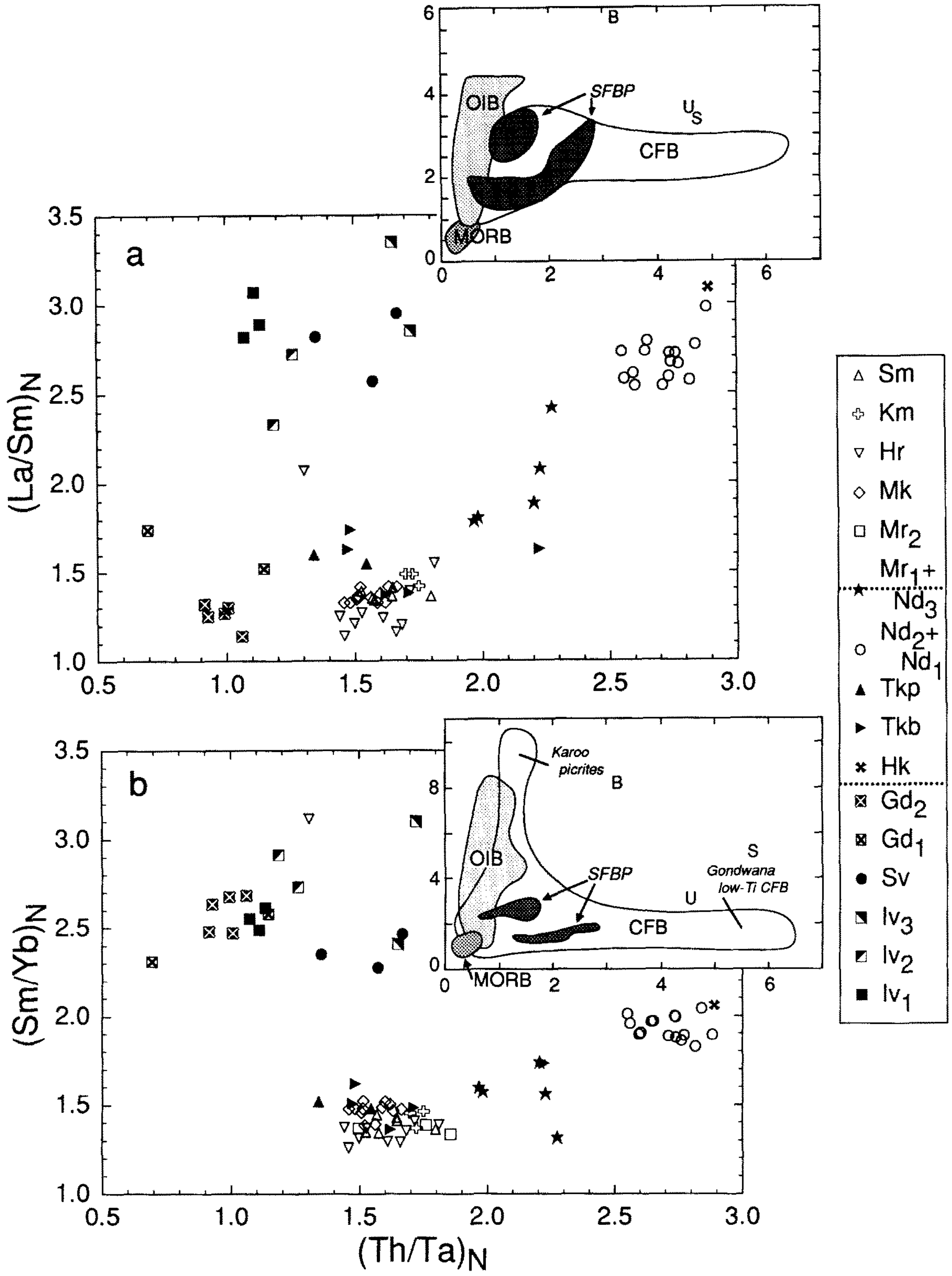

FIG. 11. (a) $(La/Sm)_N$ vs. $(Th/Ta)_N$ ratios; (b) $(Sm/Yb)_N$ vs. $(Th/Ta)_N$ ratios, compared with these ratios in other types of basalt (insets). Dotted lines in the legend separate the three basalt assemblages (see text). MORB, midoceanic-ridge basalt; OIB, oceanic-island basalt (HOFMANN et al., 1986, and K. P. Jochum, unpubl. data); CFB, continental flood basalt (CARLSON and HART, 1988; CARLSON, 1991; LIGHTFOOT and HAWKESWORTH, 1988; LIGHTFOOT et al., 1990a; MAHONEY, 1988). "Karoo picrites" (Nuanetsi picrites) from ELLAM and COX (1989, 1991); "Gondwana low-Ti CFB" (includes Tasmanian dolerites) from HERGT et al. (1989, 1991). U, ratios for average upper continental crust (CONDIE, 1993); B and S, ratios for the Bolgokhtokhsky granodiorite and upper crystalline basement, respectively, of the Noril'sk area (G. K. Czamanske, unpubl. data).

every major suite boundary and regular variation trends occur within suites (Fig. 6b). The possibility that postemplacement uranium mobility is responsible for these variations is discounted because of the systematic variation of Th/U ratios with stratigraphic position. Incompatible trace-element contents show an increase at the stratigraphic level at which the Ikonsky andesitic basalt flow was emplaced in the Kharaelaksky suite, and only slowly return to earlier, lower values (Figs. 4e, 12a). This is essentially a third example of the effects of magma mixing. The Ikonsky flow has distinct isotopic compositions but, unlike the LIL-element contents, isotopic compositions of overlying flows return immediately to values typical of the third assemblage (Fig. 6a,c). Strontium and lead isotopic compositions show significant shifts at several suite boundaries and commonly define distinct groups in the plot of $(^{87}Sr/^{86}Sr)_I$ vs. $(^{206}Pb/^{204}Pb)_I$ ratios (Fig. 9a).

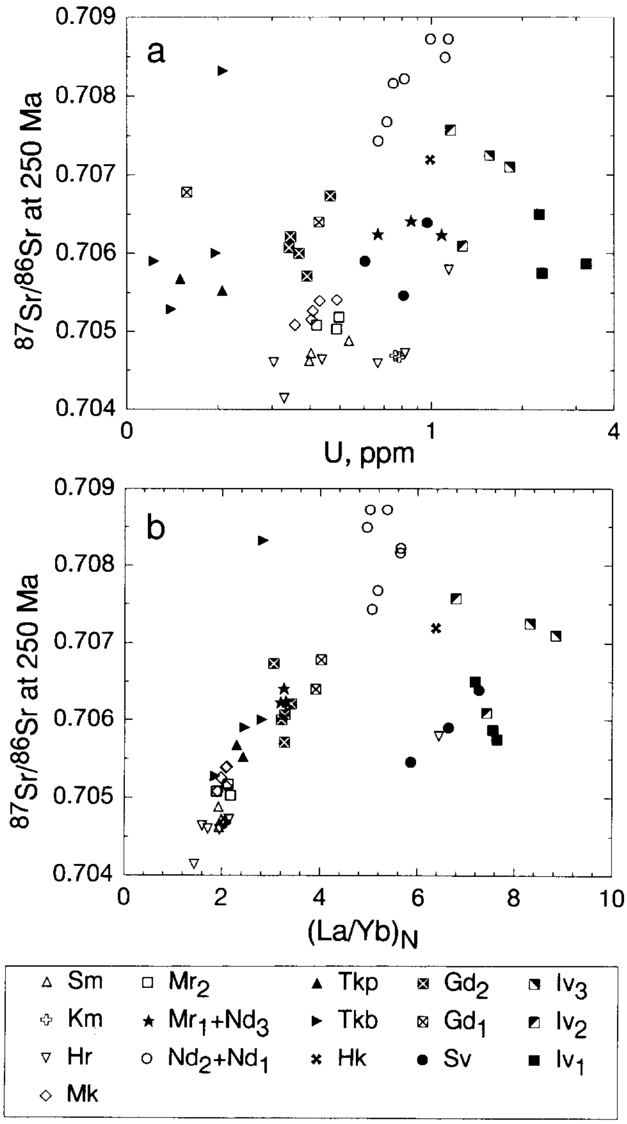

FIG. 12. (a) Uranium content vs. $(^{87}Sr/^{86}Sr)_I$ ratio; (b) $(La/Yb)_N$ vs. $(^{87}Sr/^{86}Sr)_I$ ratios.

In Fig. 11, second- and third-assemblage suites define trends that are well displaced from those of first-assemblage lavas, the main distinction being the lower $(Sm/Yb)_N$ ratios in most of the younger lavas, whose $(Sm/Yb)_N$ ratios approach those of primitive mantle and suggest that little or no garnet was residual during mantle melting. In Fig. 11a,b, one end of the trend is occupied by Tuklonsky picrites and third-assemblage basalts with low $(La/Sm)_N$ and $(Sm/Yb)_N$ and moderate $(Th/Ta)_N$ ratios ($\sim$3.5, Fig. 10), and the other by basalts of the Nd_1 and Nd_2 subsuites with intermediate $(La/Sm)_N$ and $(Sm/Yb)_N$ and very high $(Th/Ta)_N$ ratios. The increase in $(Th/Ta)_N$ ratios is accompanied by increases in SiO_2 content and $(^{87}Sr/^{86}Sr)_I$ ratios and a decrease in $\epsilon_{Nd,T}$ values. The trend is toward the compositions of continental crust, estimates of which are shown in the diagrams. The average compositions of a varied suite of upper-crustal xenoliths (S, Fig. 11 insets) from the diatreme of Morongovsky-age 25 km south of the city of Noril'sk (MASLOV and NESTEROVSKY, 1961) suggest that local crust may have had a particularly favorable composition. The overall characteristics of second- and third-assemblage lavas find parallels in the compositions of many low-Ti CFBs (DUNCAN et al., 1984; PEATE et al., 1992) and are well removed from the compositions of oceanic basalts. The relative uniformity of composition of third-assemblage basalts and the contrast they provide with first-assemblage rocks are also similar to those of other CFBs, such as the Karoo sequence, which opens with alkali volcanic rocks and picrites with varying compositions and terminates with a thick sequence of chemically monotonous basalts.

THE PLUME MODEL AND THE PETROGENESIS OF CFBs

There has been considerable recent enthusiasm for the argument that CFBs form when a starting mantle plume impinges on the base of the continental lithosphere (RICHARDS et al., 1989; CAMPBELL and GRIFFITHS, 1990; GRIFFITHS and CAMPBELL, 1990, 1991). We have chosen to analyze our data within this framework, but in no way intend to imply that other models might not be valid. A particularly favorable feature of the plume model is its ability to provide a large volume of mafic magma over a very short interval of time. We believe that the Siberian flood basalts and the ore-bearing intrusions had a common source, and our most direct evidence that this source was an asthenospheric plume comes from lead and osmium isotopic studies of the intrusions. WOODEN et al. (1992) and WALKER et al. (1993) show that the lead, neodymium, and osmium isotopic compositions of the ores and ore-bearing intrusions correspond closely to those of some Hawaiian basalts. Their osmium isotopic compositions are distinctly different from those found to characterize the lithospheric mantle beneath Siberia (PEARSON et al., 1991).

Limitations of space preclude a balanced review of the numerous models for CFB petrogenesis (we refer the reader to CARLSON, 1991), but we will address the considerable recent discussion concerning the possible significant contribution of the continental lithospheric mantle to CFB volcanism. Although numerous reports (see CARLSON, 1991) mention the possibility that the trace-element and isotopic characteristics of CFBs were acquired through assimilation of continental crust, many dismiss this possibility and conclude that such features of CFBs as high $(^{87}Sr/^{86}Sr)_I$ ratios and negative Ta-Nb anomalies are inherited directly or indirectly from sources in the continental lithospheric mantle. LIGHTFOOT et al. (1993a,b) came to this conclusion in their studies of the SFBP. An argument frequently advanced for involvement of the lithospheric mantle is that certain characteristics of CFBs are not reproduced in simple models of crust-magma interaction. Key parameters include the combination of high SiO_2 contents, high $(^{87}Sr/^{86}Sr)_I$ ratios, and negative Ta-Nb anomalies with high strontium and titanium contents, a series of attributes inconsistent with simple mixing of basalt and granite. Moreover, the typical absence of correlation of major-element compositions with trace-element abundances and isotopic compositions is inconsistent with a relatively simple model of assimilation accompanied by fractional crystallization (AFC).

Because third-assemblage basalts represent the vast bulk of SFBP magmatism, these rocks must play a central role in any model for the genesis of this province. A straightforward explanation for their relatively uniform compositions might seem to be that these magmas formed by moderate amounts of melting of a single uniform source, and in view of their volume and composition, this source is conveniently placed in the mantle. On the basis of their moderate $(^{87}Sr/^{86}Sr)_I$ ratios and $\epsilon_{Nd,T}$ values and, particularly, nearly ubiquitous negative tantalum anomalies, CFB sources in continental lithospheric mantle enriched in a "subduction component" have been advocated (cf. HAWKESWORTH et al., 1984a,b; HERGT et al., 1989, 1991; CARLSON, 1991). Starting with relatively cold lithospheric mantle, however, it is difficult to devise thermal schemes that can provide the required volumes of magma (ARNDT and CHRISTENSEN, 1992). Moreover, numerous studies of xenoliths from the continental lithospheric mantle provide no evidence that significant parts of the lithospheric mantle have been enriched in this manner or have contributed significantly to flood volcanism. In contrast, SHARMA et al. (1992) conclude that the observed geochemical and isotopic characteristics of the third-assemblage basalts of the SFBP were inherited without major changes from an asthenospheric mantle plume.

Compositions of mantle melts are controlled by the composition and mineralogy of the source and the conditions under which melting took place. The conditions under which a subcontinental plume might melt differ greatly from those associated with oceanic magmatism. The principal difference is the pressure, which profoundly influences magma composition. If the lithosphere beneath the Siberian craton had a normal thickness of ~150 km, an assumption supported by available geophysical data (ZORIN and VLADIMIROV, 1989), the pressure at its base would have been about 50 kbars. Thermomechanical modelling by ARNDT and CHRISTENSEN (1992) has shown that during plume-lithosphere interaction, erosion of the lithosphere is generally small and most melting takes place at sublithospheric depths and pressures. Magmas formed under these conditions, even those formed by melting close to the peridotite solidus, would be highly magnesian. Parameterization of available, high-pressure experimental data (e.g., TAKAHASHI, 1986, 1992; HERZBERG et al., 1990) using a procedure similar to that of MCKENZIE and BICKLE (1988) yields an MgO content of 22–24 wt% for low-percentage partial melts at 50 kbars (M. J. Cheadle, pers. commun., 1993). We stress this fact because it is critical to the following interpretation of the genesis of CFBs. During ascent through the lithospheric mantle, asthenospheric magmas may react with peridotitic wall rocks, the most notable modification of their composition being the crystallization of olivine and consequent decrease in MgO content. If major-element equilibrium were reached between magma and wall rock, the MgO content of the magma when it arrives at the base of the crust will be similar to that of peridotite at ambient subcrustal pressures. At 12–15 kbars, such melts will contain 12–15 wt% MgO according to the MCKENZIE and BICKLE (1988) parameterization. However, we consider it unlikely that low-viscosity melts, rapidly ascending by fracture propagation (NICOLAS, 1986, 1989; SPENCE and TURCOTTE, 1990), will fully equilibrate with the lithosphere (see discussion by HUPPERT and SPARKS, 1985) and suggest that these melts reached the Moho with MgO contents of 15 wt% or more.

These primary plume-derived melts would have been in equilibrium with garnet, as well as olivine, orthopyroxene, and clinopyroxene, and this assemblage would leave a distinctive trace-element imprint, expressed by a characteristic depletion in HREEs. If the partial-melt fractions were low, the melts would have high contents of incompatible elements; the first-assemblage Ivakinsky and Syverminsky suites have all these characteristics. With increasing percentages of melting, the contents of incompatible elements would decline, and MgO content would increase, though not dramatically. Eventually, garnet would be exhausted, and the trace-element pattern would lose its HREE depletion; these features characterize second- and third-assemblage magmas. The Gudchikhinsky suite represents tholeiitic and picritic magmas with flat LREE patterns but depleted HREEs, i.e., patterns that basically combine the trace-element characteristics found in the lower part of the first assemblage with those of the second- and third-assemblage lavas. Because the Gudchikhinsky suite lies stratigraphically between the Ivakinsky and Syverminsky suites and second-assemblage lavas, a possible explanation for its geochemical characteristics is that it represents transitional melting conditions. In contemplating this transition, we note that there is no indication of a significant time break during SFBP volcanism. We offer two suggestions: (1) magmas parental to the first assemblage may have been generated as the plume head was en route to its highest level, or (2) in response to the plume, the continental lithospheric mantle may have been thinned by extension or thermal erosion, allowing the plume to ascend to a shallower level by the time of Tuklonsky magmatism.

Some isotopic and trace-element constraints for the plume source can be estimated from the compositions of OIBs and from the studies of the ores and ore-bearing intrusions. The lead, neodymium, and osmium isotopic compositions reported by WOODEN et al. (1992) and WALKER et al. (1993)

indicate that, with respect to those systems, the plume source region was similar to that for Hawaiian basalts. Although OIBs define large fields in traditional isotopic diagrams (e.g., HART et al., 1992), they do not display the more extreme compositions—in particular, high $(^{87}Sr/^{86}Sr)_I$ ratios and low $\epsilon_{Nd,T}$ values—that characterize many CFBs and samples from the continental lithospheric mantle (Fig. 8a). CFBs are distinguished from OIBs and midoceanic-ridge basalts (MORBs) by a key trace-element parameter—negative Ta-Nb anomalies are present in most CFBs, but are absent, or extremely rare and small, in oceanic basalts (Fig. 11; e.g., ARNDT and CHRISTENSEN, 1992, their Fig. 4). The SFBP is underlain by a thick sequence of Paleozoic carbonates, evaporites, and arenaceous sedimentary rocks, a gneissic basement of Precambrian age, and a thick continental lithospheric mantle. Melts generated in the asthenosphere would have traversed all of these rocks during their ascent and may have interacted with them during periods of ponding; each is a possible contaminant. However, elevated $(^{87}Sr/^{86}Sr)_I$ ratios, low $\epsilon_{Nd,T}$ values, unradiogenic lead isotopic compositions, and especially negative Ta-Nb anomalies point to old continental crust as the most significant contaminant.

The following arguments indicate that derivation of the Siberian flood basalts directly from the mantle, whether asthenospheric or lithospheric, is not tenable. First, and most powerful, is the uniform, yet highly evolved, composition of most third-assemblage basalts. With MgO contents near 7 wt% and Mg# of 50–55, these are not primary mantle melts—their compositions are far removed from magmas formed by the melting of mantle at sublithospheric depths. The crystallization of at least 30% olivine is required to derive a basalt containing 7 wt% MgO from a primary magma containing more than 20 wt% MgO, as would have formed by melting of mantle peridotite at pressures prevailing at the base of the continental lithosphere ($\sim$50 kbars). Even if the effects of extensive interaction between the primary melts and lithospheric mantle are allowed, the magmas reaching the Moho would contain at least 12–15 wt% MgO. Thus, additional evolution must have taken place in the crust, an observation supported by consideration of the mineralogy and chemical compositions of the erupted basalts. Phenocrystic plagioclase in many flows and aspects of their major-element compositions, such as nearly constant Al_2O_3 contents and decreasing CaO with decreasing MgO contents, indicate that plagioclase and clinopyroxene have also fractionated. The minimal change in $(Gd/Yb)_N$ that accompanies relatively constant Al_2O_3 contents in third-assemblage basalts indicates that garnet was not present in the fractionating assemblage. The presence of plagioclase and an absence of garnet is evidence that the fractionation took place at pressures less than 9 kbars (depths less than about 30 km; WINTHER and NEWTON, 1990; RAPP and WATSON, 1993).

Whereas these arguments indicate that fractionation of the mantle-derived melts took place within the continental crust, this fractionation was not haphazard. During the evolution of the third-assemblage basalts, the major-element abundances were buffered so efficiently that only magmas with a restricted range of compositions escaped the reservoir and reached the surface. The relatively uniform major-element compositions are therefore not an argument for a source of uniform composition, and the same is also true for those trace elements influenced by the fractionation of olivine, clinopyroxene, or plagioclase.

The second argument hinges on strontium abundances, which are moderate in third-assemblage basalts and high in the Nd_1 and Nd_2 subsuites. Unlike many CFBs, which have negative strontium anomalies that are readily attributable to plagioclase fractionation, the Siberian flood basalts have negligible or positive anomalies on mantle-normalized plots (Fig. 5). The absence of negative strontium anomalies in rocks that have fractionated plagioclase indicates either an excess of strontium in the parental magma or contamination with Sr-rich material. Although it might be argued that high strontium content is an expected feature of a lithospheric mantle enriched with "subduction component," such a source should also have high cesium, rubidium, and barium contents (e.g., WHITE and PATCHETT, 1984; SUN and MCDONOUGH, 1989). This is not apparent in the Siberian flood basalts. The Bolgokhtokhsky granodiorite, which crops out 50 km west of Noril'sk and presumably formed by partial melting of lower crustal rocks, contains 1,600 to 1,700 ppm Sr. Among others, HILDRETH and MOORBATH (1988) have shown the potential for assimilation of lower-crustal materials to elevate the strontium contents of mantle-derived melts. For rocks of the Nadezhdinsky suite, positive correlations between strontium content and indices of crustal contamination, such as $(Th/Ta)_N$ and $(^{87}Sr/^{86}Sr)_I$ ratios and $\epsilon_{Nd,T}$ values, provide evidence of contamination with Sr-rich material. Thus, the strontium contents of the Siberian basalts, rather than indicating a mantle origin, appear to provide an indication of the geochemical characteristics of their crustal contaminants and processing.

Finally, there is no evidence for the common existence of a subduction-enriched component in the continental lithospheric mantle, let alone beneath CFB provinces. Although material apparently is transported from subducted oceanic crust into the mantle wedge overlying subduction zones, there is no compelling evidence that this mantle wedge is typically transformed into lithospheric mantle. Although evidence for a "subduction component" has been found in analyses of xenoliths from the mantle beneath island arcs (MAURY et al., 1992), complications of analyses of ultramafic nodules from the continental lithospheric mantle show few of the distinctive features of this component: e.g., negative Ta-Nb anomalies and enrichment in LIL elements are absent (e.g., MCDONOUGH, 1990, 1992; MENZIES, 1992). The well-publicized, but relatively rare, metasomatized peridotite nodules, which are enriched in incompatible elements and have radiogenic isotopic compositions, have negligible or positive Ta-Nb anomalies. This type of metasomatism is best related to influx of low-percentage melts (HAWKESWORTH et al., 1984b; MENZIES et al., 1987). It is interesting to speculate that if the Siberian continental lithospheric mantle had indeed formed in a subduction environment and at one time had a crustal geochemical signature, this signature has been overwhelmed in this Precambrian lithospheric mantle by a continuous, billion-year-long influx of low-melt fractions from the underlying asthenosphere.

THE ROLE OF A MAGMA RESERVOIR THAT IS PERIODICALLY REPLENISHED, PERIODICALLY TAPPED, AND CONTINUOUSLY FRACTIONATING DURING ASSIMILATION OF CRUSTAL WALLROCK

Our interpretation of the data for the Noril'sk lava sequence requires four distinct magma types—one for each of the assemblages, with the Gudchikhinsky picrites representing a fourth type which was transitional between that represented by the two earlier suites of the first assemblage and that represented by the second assemblage. There is indication of two major periods of mixing between strongly fractionated + contaminated magma and more weakly contaminated + fractionated magma—one in the Syverminsky suite and another within the Nadezhdinsky suite, associated with the transition from second- to third-assemblage basalts. Fractionation affected all magmas significantly—none have MgO contents close to possible primary mantle melts—and some of the magmas to a high degree (e.g., the Iv_2, Iv_3, Nd_1, and Nd_2 subsuites). Variations in isotopic compositions within suites and correlation of isotopic ratios with SiO_2 contents indicate that contamination has obviously accompanied fractionation in several specific cases and probably plays at least some role in all cases.

We propose that the geochemical and petrologic variations observed within the SFBP can be explained in terms of a model that combines (1) temporal evolution in the composition of mantle-derived magma, a feature that is consistent with a mantle-plume source, and (2) processing in the crust, which involves modifying the compositions of these different magma types through regulation of magma throughput, crystal fractionation, and assimilation/partial melting of crustal rocks. We recognize the possibility that the magmas interacted with, or were contaminated with, material from the continental lithospheric mantle. Indeed, there is moderately convincing evidence of such a process in other regions (ELLAM et al., 1992). However, at present these processes are not well understood and we prefer to attribute the "crustal" signature of CFBs to crustal contamination. We therefore propose that fractionation and contamination in a dynamic magma reservoir in the lower continental crust was the dominant control on the geochemical characteristics of third-assemblage basalts and the Nd_1 and Nd_2 subsuites.

A series of reports by O'HARA (1977, 1980; O'HARA and MATHEWS, 1981) described geochemical evolution in a magma reservoir that is periodically replenished and tapped, while undergoing continuous fractionation and assimilation of its wallrocks (RTFA). Although we emphasize here the work of M. J. O'Hara because of our interest in examining quasi-quantitative relations associated with such a reservoir, the melting, assimilation, storage, and homogenization (MASH) process of HILDRETH and MOORBATH (1988) is comparable in concept. O'HARA (1977) pointed out that magmas erupting from RTFA magma reservoirs will differ markedly from magmas affected only by fractional crystallization or simple mixing because their compositions depend on the relative rates of magma replenishment, tapping, and fractionation, and on the extent of wallrock assimilation. We also consider here a variant to the RTFA model because, in addition to bulk assimilation of country rocks, partial melts of the crust probably are locally produced by the influx of extremely large volumes of mafic magma. Such partial melts may constitute a significant proportion of the material that is assimilated and mixed into the fractionating magmas. If the main variables in the RTFA process are held approximately constant and a steady state is approached, the erupted lavas should display ". . . (1) uniformity of composition . . . ; (2) large differences of composition between the lava and the parental magma with respect to major and trace element contents and ratios; (3) strong control of liquid composition by the low pressure phase equilibria . . ." (O'HARA, 1977, p. 507). These are important features of the SFBP and other CFBs.

In Table 3, we demonstrate the feasibility of this process by modeling the generation of (a) typical basalt from the voluminous third assemblage and (b) an average basaltic composition for the heavily contaminated Nd_1 subsuite. The parental magma in both cases was based on the composition of the Tuklonsky picrites, but with a relatively flat pattern of mantle-normalized trace elements. Three contaminants were considered. Contaminant 1 has a composition based on CONDIE's (1993) average upper continental crust (for all elements except tantalum and thorium, this composition is comparable to that of TAYLOR and MCLENNAN's (1985) upper continental crust); it was used to model bulk assimilation of felsic material (either granitoid or metasedimentary) or a partial melt of granitic composition by the parental magma. The strontium content is relatively high (1,000 ppm), though lower than the 1,600–1,700 ppm found in the Bolgokhtokhsky granodiorite, a local pluton (see the following text) that has previously been used in contamination models (LIGHTFOOT et al., 1993a,b). Contaminant 2 has a mafic composition based on RUDNICK and PRESPER's (1990) average composition of lower crustal xenoliths, but with lower Ta/La ratio. In this rather extreme case, we model bulk contamination with metabasalt that might constitute a mafic underplate of the lower continental crust. Contaminant 3 has a tonalitic composition based on a series of 8-kbar partial-melting experiments on metabasalt (RAPP et al., 1991). The major-element composition was based on the averages from their experiments, and the trace-element contents were estimated from the data of RAPP et al. (1991, Fig. 6). In this case, we model selective contamination with a low-melting fraction from a mafic source. A more evolved isotopic and LIL-element composition was used for the granitoid contaminant of the Nadezhdinsky basalt ($(^{87}Sr/^{86}Sr)_I = 0.710$, $\epsilon_{Nd,T} = -20$) than for the contaminants of the third-assemblage basalts ($(^{87}Sr/^{86}Sr)_I = 0.707$, $\epsilon_{Nd,T} = -3$).

The compositions were calculated by using the equations of O'HARA (1977). Isotopic compositions were modeled by assuming the same distribution coefficient for each isotope—i.e., no isotopic fractionation was attributed to processes in the magma reservoir. Input, fractionation, and contamination parameters, as well as elemental-distribution coefficients (D), are listed in Table 3. The approach has much in common with that adopted by COX (1988), who modeled the generation of flood basalts in an RTF magma reservoir but did not incorporate the assimilation of crustal rocks, a process we believe to be of fundamental importance. The open-system variant suggested by BRÜGMANN et al. (1993) on the basis of siderophile and chalcophile metal analyses of the SFBP sample suite analysed by LIGHTFOOT et al. (1990b, 1993a) does incorporate contamination and is akin to our model.

Table 3 shows that the calculated and measured compositions agree well, including reproduction of the enrichment in SiO_2 and incompatible trace elements and of the isotopic compositions. The high strontium content of the hybrid magmas is maintained, and a negative tantalum anomaly is introduced. The slight mismatches for the HREEs (reflected by samarium and ytterbium contents) would be improved by adopting a lower $(Sm/Yb)_N$ ratio in the parental magma of the third-assemblage basalts, a change consistent with general evolution within the lava pile. There is also a mismatch for nickel in the Nadezhdinsky modelling, probably resulting from sulfide-melt fractionation (NALDRETT et al., 1992; BRÜGMANN et al., 1993), a process not considered in the calculations.

The fit for the third-assemblage basalts is equally good for all three contaminants, but the calculated amount of assimilated mafic crust is improbably high, at 62%. For this reason, a model of selective assimilation of partial melts of mafic crust is probably most reasonable if the reservoir was resident in rocks of basaltic composition. Even in this case, however, the tantalum anomaly poses a problem. To reproduce the tantalum anomaly observed throughout the basalt sequence requires a $(Ta/La)_N$ ratio in the contaminant of about 0.4, far lower than that recorded in suites of mafic xenoliths—RUDNICK and PRESPER (1990) found an average value of 0.8. However, the generally high strontium contents in mafic xenoliths, which RUDNICK (1992) attributed to the presence of cumulus plagioclase, coincides well with the need for a contaminant with high strontium content for the Siberian basalts.

These results were obtained with a choice of input parameters that we believe to be reasonable. For example, for Y (the fraction of liquid extracted as a lava flow at the end of each cycle), we used a value of 0.002 for the third-assemblage basalts and 0.01 for the Nadezhdinsky basalts. According to these parameters, the average thickness of a Siberian flood-basalt flow, earlier estimated at 15 m, would relate to a magma reservoir that was effectively 1.5 km thick during production of Nd_1 and Nd_2 basalts and to a reservoir that was effectively 7.5 km thick during production of third-assemblage basalts. The larger reservoir responsible for the third assemblage was situated where the ascending mafic magmas reached a point

Table 3. Formation of flood basalts in RTFA magma chambers.

	Th	Ta	La	Pb	Sr	Nd	Sm	Yb	Ni	SiO_2	Al_2O_3	FeO	MgO	CaO	$^{87}Sr/^{86}Sr$	$^{143}Nd/^{144}Nd$	$^{206}Pb/^{204}Pb$
Third-assemblage basalt																	
Parent	0.2	0.1	2.1	0.6	60	4.0	1.3	1.2	500	47.0	10.0	11.0	16.0	11.0	0.7030	0.51280	18.00
Contaminant 1	5.7	0.8	30	17	1000	26	4.5	2.2	20	66.0	15.0	4.5	2.2	3.5	0.7070	0.51250	17.40
Contaminant 2	1.6	0.6	13	2.0	422	15	3.5	1.9	100	50.5	16.5	9.1	7.7	10.0	0.7070	0.51250	17.40
Contaminant 3	4.0	0.5	24	12	800	19	5.0	3.0	10	68.0	17.0	4.0	1.0	3.0	0.7070	0.51250	17.40
Model basalt 1	1.4	0.37	9.0	4.0	194	12	3.2	2.1	130	49.9	15.6	12.2	7.8	11.0	0.7052	0.51271	17.77
Model basalt 2	1.2	0.48	9.6	2.1	189	14	3.7	2.4	129	49.2	15.9	12.8	7.7	10.8	0.7054	0.51266	17.49
Model basalt 3	1.2	0.30	8.2	3.3	190	11	3.2	2.2	127	50.8	15.9	11.8	7.4	11.4	0.7052	0.51271	17.85
Measured basalt	1.2	0.32	8.6	2.0	200	13	3.8	2.8	130	49.4	15.4	12.0	7.1	11.4	0.7051	0.51267	17.80

Contaminant 1 (granitoid)				Contaminant 2 (mafic)				Contaminant 3 (tonalitic)			
Input parameters		Proportions of phases		Input parameters		Proportions of phases		Input parameters		Proportions of phases	
X	0.0014	ol	0.50	X	0.0015	ol	0.45	X	0.0012	ol	0.55
Y	0.001	cpx	0.35	Y	0.001	cpx	0.35	Y	0.001	cpx	0.30
q	0.10	plag	0.15	q	0.10	plag	0.20	q	0.15	plag	0.15
Proportion of contaminant	6%			Proportion of contaminant	62%			Proportion of contaminant	9%		

	Th	Ta	La	Pb	Sr	Nd	Sm	Yb	Ni	SiO_2	Al_2O_3	FeO	MgO	CaO	$^{87}Sr/^{86}Sr$	$^{143}Nd/^{144}Nd$	$^{206}Pb/^{204}Pb$
Nadezhdinsky basalt																	
Parent	0.2	0.1	2.1	0.6	60	4.0	1.3	1.2	500	47.0	10.0	11.0	16.0	11.0	0.7030	0.51280	18.00
Contaminant	5.7	0.8	40	7.0	1200	35	6.6	2.9	100	66.0	15.0	4.5	2.2	3.5	0.7100	0.51155	17.50
Model basalt	2.5	0.56	17.8	4.0	341	19.1	4.5	2.6	114	52.8	15.8	10.2	7.1	9.8	0.7084	0.51210	17.60
Measured basalt	3.1	0.49	17.2	3.9	310	18	3.9	2.1	45	53.0	15.3	9.5	6.9	10.1	0.7085	0.51210	17.60

Input parameters		Proportions of phases	
X	0.014	ol	0.55
Y	0.010	cpx	0.25
q	0.25	plag	0.20
Proportion of contaminant	15%		

Distribution coefficients (D; all calculations)

	Th	Ta	La	Pb	Sr	Nd	Sm	Yb	Ni
ol	.001	.001	.001	.001	.001	.001	.001	.010	10.0
cpx	.002	.020	.050	.050	.100	.200	.300	1.0	1.0
plag	.001	.001	.001	.001	2.0	.001	.001	.020	0.0

Explanation: 1. Composition of steady-state liquid, calculated using the equation $\frac{Cb}{Co} = \frac{\{X[1+g((Cg/Co)-1)]+Y\}(1-X)^{(D-1)}}{1-(1-X-Y)(1-X)^{(D-1)}}$ from O'Hara (1977).

a. Input parameters — X - mass fraction of cumulate formed in each cycle.
Y - mass fraction extracted as a lava flow.
q - fraction of total cumulate precipitated to provide the energy to digest wall rocks

b. Proportions of phases — Mass fraction of olivine, clinopyroxene, and plagioclase in fractionating assemblage

c. Proportion of contaminant — Represents proportion of contaminant in steady-state liquid, calculated from mass balance.

of neutral buoyancy in the lower crust, perhaps near the discontinuity represented by the crust-mantle interface (FURLONG and FOUNTAIN, 1986). The smaller reservoir, whence the Nadezhdinsky basalts were derived, may have been at this level or, more likely, given the need for a more isotopically evolved contaminant, at a midcrustal level. There is little evidence as to whether the lower crust of this poorly known area was composed of underplated mafic rocks or relatively felsic granulites, but the materials contributed to the RTFA reservoir may have been comparable in either case. Low-percentage partial melting of relatively mafic rocks has been shown to produce tonalitic liquids (RAPP et al., 1991; RAPP and WATSON, 1993), whose incorporation could produce effects comparable to those that might be expected from bulk assimilation of more felsic crust.

We emphasize that the particular model parameters listed in Table 3 are by no means unique, and that similar agreements can be obtained by using different input parameters. For example, the absolute values of parameters X and Y do not control the composition of the steady-state magma; only the ratio is important. We chose small values in the case of third-assemblage basalts mainly because a large reservoir is more likely to yield basalts of relatively uniform composition. We used an MgO content of 16 wt% for the mantle-derived magmas fed into the RTFA reservoir. This represents a decrease of 4–9 wt% from the MgO contents considered typical of primary magmas derived from a plume impinging on the base of the continental lithosphere (TAKAHASHI, 1986, 1992), a decrease that is attributed primarily to olivine fractionation as these magmas ascended through the pyroxene-bearing lithospheric mantle. As noted earlier, it is possible that fractionation and interaction with the lithospheric mantle during transit could result in even lower MgO contents for the input magmas and notable modification of isotopic and trace-element characteristics. If, however, the MgO contents were too low (less than about 12 wt%), it becomes impossible to produce the major-element, trace-element, and isotopic compositions of the erupted basalts using realistic parameters. We believe the qualitative parameters used in this model to be plausible, and report these results to illustrate that processes in a crustal magma reservoir can produce the critical characteristics of flood basalts, including their highly evolved yet relatively uniform major-element compositions, a decoupling of the major-element compositions from trace-element and isotopic compositions, and the imposition of crustal trace-element and isotopic characteristics. On the basis of isotopic and incompatible-element data, PENG et al. (1993) came to a similar conclusion in their study of the lower six formations of the western Deccan Traps. The Ivrea Zone of northern Italy contains mafic intrusions that are postulated to represent magma reservoirs which have operated much as we propose (e.g., VOSHAGE et al., 1990).

One or more dynamic RTFA reservoirs in which magma throughput varied substantially may explain some of the intriguing elemental and isotopic correlations in the Noril'sk lava sequence. An example may be the good positive correlation between $(La/Yb)_N$ and $(^{87}Sr/^{86}Sr)_I$ ratios shown by all second- and third-assemblage samples (Fig. 12b). Although the parental magmas for the two assemblages seem to have some specific compositional differences (e.g., LIL-element contents), their primary $(La/Yb)_N$ and $(^{87}Sr/^{86}Sr)_I$ ratios would have been similar if both were produced by high-percentage partial melting of a common mantle source and underwent a similar amount of RTFA processing. RTFA processing of Tuklonsky-like, second-assemblage magmas, involving extensive assimilation, would increase $(La/Yb)_N$ and $(^{87}Sr/^{86}Sr)_I$ ratios to the high values observed in the Nd_1 and Nd_2 subsuites. Magma input to the reservoir would have been low at this stage. Magma mixing between the highly modified Nd_1 and Nd_2 magmas and a less modified third-assemblage magma would scatter compositions back along the RTFA trend, during a stage representing greatly increased magma input to the reservoir. If the contents of an incompatible element, rather than an elemental ratio, are used in comparable plots (e.g., uranium vs. $(^{87}Sr/^{86}Sr)_I$, Fig. 12a), the strongly LIL-element-depleted, second-assemblage Tuklonsky magmas are distinguishable from the third-assemblage magmas, and separate RTFA and magma-mixing trends are recognizable. Even the fact that there is no simple relation between the isotopic compositions of the picritic and basaltic lavas of either the Gudchikhinsky or Tuklonsky suites is most understandable if the magmas to these suites were undergoing complex processing in a reservoir from which cumulus olivine could be entrained.

Because of the fundamental differences in melting conditions discussed earlier, both elemental contents and elemental ratios are distinct in (1) first-assemblage magmas and (2) second- and third-assemblage magmas. Almost any elemental-variation diagram will distinguish these two groups. Isotopic differences among the least modified members of all three assemblages, however, are not so distinct (e.g., Figs. 7, 8, 9), and isotopic-variation diagrams alone will not always identify their fundamental petrogenetic differences. This characteristic of SFBP magmatism is consistent with imposition of most of the isotopic variations on parental magmas by RTFA processing. In view of the complexity of the system and the processing that we believe the magmas to have undergone, we consider it premature to speculate on the heterogeneity of the plume source with respect to the various isotopic systems. We think that the parental melts represent a common plume source with minimal isotopic variation. On the basis of the combined lead and osmium isotopic studies (WALKER et al., 1992, 1993), there is reason to believe that this source was characterized by subtle isotopic heterogeneity.

ISOTOPIC COMPOSITION AND AGE OF THE CRUST INVOLVED IN SFBP MAGMATISM

There is evidence that the crustal components involved in Noril'sk-area magmatism had a range of isotopic compositions and that the basalt sequence reveals a temporal pattern to isotopic variation in the contaminant. The silica-rich members of the Iv_2 and Iv_3 subsuites and the Syverminsky suite provide the first evidence for the isotopic compositions of a crustal contaminant. At 250 Ma, its $^{87}Sr/^{86}Sr$ ratio must have been 0.708 or greater, its ϵ_{Nd} value −4 or lower, and its lead isotopic composition moderately unradiogenic (Table

4; Figs. 7, 8, 9). If the isotopic compositions of the Tuklonsky tholeiites and picrites also reflect crustal contamination, then a component with strongly unradiogenic Pb-isotopic compositions is required (Table 4); however, its $^{87}Sr/^{86}Sr$ ratio (0.706 or higher) could be lower than that involved in the evolution of the Ivakinsky subsuites, whereas its ϵ_{Nd} value would have been about the same.

The highly modified Nd_1 and Nd_2 subsuites require that the isotopic composition of the contaminant varied during their eruption. The lowermost flow in the Nd_1 subsuite indicates a contaminant with isotopic compositions similar to those suggested by the upper Ivakinsky subsuites, except that a much more extreme ϵ_{Nd} value of -11 or less is required. However, the immediately overlying Nd_1 flows require a slightly higher $^{87}Sr/^{86}Sr$ ratio (0.709 or greater), a possibly less negative ϵ_{Nd} value (-8), and more radiogenic lead isotopic compositions (Table 4). The strontium and neodymium isotopic characteristics indicated by Nd_2 samples remain unchanged, but the lead isotopic compositions indicated are less radiogenic, seemingly moving back toward values like those seen in the upper Ivakinsky and lowermost Nd_1 samples. Third-assemblage samples indicate a contaminant similar to that reflected in the composition of the Tuklonsky suite—one with strongly unradiogenic lead isotopic compositions, low $^{87}Sr/^{86}Sr$ ratios, and moderate ϵ_{Nd} values (Table 4).

Models that could reproduce the implied range of isotopic compositions may involve varying the crustal level at which assimilation occurred and, thus, the metamorphic grade and/or bulk composition of the crust involved. A high-grade, U- and Rb-depleted lower crust would provide the unradiogenic lead and strontium isotopic compositions; a similar crustal source is also necessary to account for the characteristics of some of the Deccan basalts (PENG et al., 1993). Crust with a mafic bulk composition could also provide these features, with the added advantage of also providing moderate ϵ_{Nd} values, because it would be more likely to have only a moderately fractionated REE pattern and low $(Th/Ta)_N$ ratios. The more radiogenic lead and strontium isotopic compositions and more negative ϵ_{Nd} values imply lower-grade, middle crust of probable intermediate to felsic composition, displaying strongly fractionated REE patterns and high $(Th/Ta)_N$ ratios.

Both the unradiogenic lead isotopic compositions and the ϵ_{Nd} values of -8 to -11 provide general age information about possible crustal contaminants, because initial lead isotopic compositions and ϵ_{Nd} values will be too high in more recently formed, juvenile crust. An ϵ_{Nd} value of -11 or lower suggests juvenile crust formed in or before the Early Proterozoic. The lead isotopic compositions are generally consistent with a Middle Proterozoic or older crust with long-term average $^{238}U/^{204}Pb$ and $^{232}Th/^{204}Pb$ ratios significantly less than those of average crust, but a long-term average Th/U ratio slightly higher than that of average crust. These U-Th-Pb characteristics are consistent with a mafic to felsic, high-grade, lower crust, but are not necessarily restricted to that crustal environment.

Little is known, unfortunately, about the specific isotopic characteristics of the crust that underlies the Noril'sk area. Limited lead isotopic data on crustal xenoliths from the Morongovsky-age diatreme south of Noril'sk are consistent with at least some of the crust being Early Proterozoic and having lead isotopic compositions appropriate for the proposed contaminant (J. L. Wooden, unpubl. data). The Bolgokhtokhsky granodiorite, 50 km west of Noril'sk and interpreted as a melt of the lower crust, has been specifically suggested as representing a possible contaminant composition for the Nd_1 and Nd_2 magmas (LIGHTFOOT et al., 1993a,b). With an age of ~222 Ma (G. B. Dalrymple, unpubl. data based on $^{40}Ar/^{39}Ar$ dating of biotite and amphibole), its lead isotopic compositions are retarded $[(^{206}Pb/^{204}Pb)_I = 16.29$, $(^{207}Pb/^{204}Pb)_I = 15.30$, $(^{208}Pb/^{204}Pb)_I = 36.70]$, but its $(^{87}Sr/^{86}Sr)_I$ ratio is only 0.70634 (J. L. Wooden, unpubl. data), much too low for achieving the strontium isotopic shift required of a suitable contaminant. The granodiorite has an ϵ_{Nd} value of -14 and chondritic osmium isotopic characteristics (WALKER et al., 1993). Thus, if our assumption about its derivation is correct, its lead and neodymium isotopic compositions support our interpretation that the lower crust contains Early Proterozoic and older rocks.

A cautionary note is required about the interpretation of isotopic compositions of possible mantle source regions for the Noril'sk lava sequence and for CFBs in general. Other workers have attempted to evaluate these compositions and have emphasized the initial isotopic compositions of the relatively homogeneous third-assemblage basalts (DEPAOLO and WASSERBURG, 1979; SHARMA et al., 1991, 1992). This study and those by LIGHTFOOT et al. (1990b, 1993a,b) have provided a wealth of information indicating the complexity of the entire magmatic system in the Noril'sk area. Although the third-assemblage suites appear simple, significant and regular trace-element and isotopic variations exist even in these studies. Their limited major-element variations also can be interpreted as the result of complex processes involving significant fractionation and contamination that occurred in or at the base of the crust (the RTFA model described above). It appears extremely unlikely that any magmas represented in the Noril'sk lava sequence reached the surface with elemental or isotopic compositions unmodified from those of their parental, mantle-derived melts. Even with a better understanding of possible crustal contaminants and the specific

Table 4. Limiting isotopic compositions of possible contaminants of the SFBP at 250 Ma.

Lavas	$^{87}Sr/^{86}Sr$	ϵ_{Nd}	$^{206}Pb/^{204}Pb$	$^{207}Pb/^{204}Pb$	$^{208}Pb/^{204}Pb$
Iv_2, Iv_3, and Sv	≥0.708	≤-4	≤17.3	≤15.42	≤37.3
Tk	≥0.706	≤-4	≤16.8	≤15.39	≤36.9
Lowermost Nd_1	≥0.708	≤-11	≤17.3	≤15.42	≤37.3
Remaining Nd_1	≥0.709	≤-8	≥17.7	≥15.47	≥37.7
Nd_2	≥0.709	≤-8	≤17.3	≤15.42	≤37.3
Third assemblage	≥0.706	≤0	≤17.6	<15.43	<37.6

nature of the several operative modification processes, it seems that only general constraints can be placed on the primary, mantle isotopic compositions. A comparable call for caution in inferring mantle-source characteristics from the isotopic compositions of continental basalts was issued by RUDNICK et al. (1986) on the basis of their study of lower-crustal xenoliths.

GENERAL CONSIDERATIONS

We suggest that the concepts presented in the preceding text are generally applicable in the context of the mantle-plume model for the origin of CFBs. Where the lithosphere is thick, melting within the plume will take place at relatively high pressure in the presence of garnet, and the percentage of melting will be relatively low. Such conditions produce the parental magmas of high-Ti-K basalts. Where and when the lithosphere is thinner, the plume may ascend to shallower levels, with the result that the percentage of melting will be greater. Garnet may be exhausted, and the magmas will contain relatively low contents of moderately to highly incompatible trace elements. These magmas may be parental to low-Ti-K basalts. Processing in RTFA magma reservoirs may well be the norm. This processing imposes a crustal signature on the magmas, as expressed most strongly by low $(Ta/La)_N$ ratios and evolved isotopic compositions; the overall characteristics of the parental magma will be retained in the contents of moderately compatible elements (e.g., titanium).

We recognize that this model cannot explain the evolution of all the lavas in CFB sequences. The Nuanetsi picrites of the Karoo province in South Africa, for example, remain a problem. Certain features of those rocks, such as the presence of large negative Ta-Nb anomalies in samples with very high contents of incompatible elements and high MgO contents (ELLAM and COX, 1989, 1991), or the positive correlation between $\epsilon_{Nd,T}$ and γ_{Os} values (ELLAM et al., 1992), appear to require some type of interaction between a picritic parental magma and continental lithospheric mantle, as discussed by ELLAM and COX (1991) and ARNDT and CHRISTENSEN (1992). For nearly all CFBs, however, the hypothesis that the crustal signature is largely imposed in an RTFA magma reservoir holds promise, as discussed in more depth by ARNDT et al. (1993).

CONCLUSIONS

The geochemical and isotopic characterizations of the SFBP in the Noril'sk area presented here and by LIGHTFOOT et al. (1990b, 1993a) are in excellent agreement. We concur with many of the detailed petrologic inferences that LIGHTFOOT et al. (1990b, 1993c) made from their data, e.g., that extensive crustal contamination was involved in the formation of the Nadezhdinsky lavas. However, we disagree that the lithospheric mantle was significantly involved in SFBP magmatism (LIGHTFOOT et al., 1993a); instead we favor the processing of magmas derived from an asthenospheric mantle plume in crustal RTFA reservoirs. The formulation of our model was greatly influenced by the relatively monotonous compositions of the voluminous third-assemblage basalts, only the lower 20–25% of which were represented in the studies of LIGHTFOOT et al. (1990b, 1993a).

The major conclusions of our study are as follows:

1) The elemental and isotopic compositions of the Siberian CFBs are far removed from those of their asthenospheric-mantle sources.
2) The dominant source of erupted magma was a mantle plume. The compositions of the primary magmas were controlled by the thickness of the lithosphere, which influenced the depth of melting, the residual mineral assemblage, and the percentage of melting in the source region.
3) The observed chemical and isotopic characteristics of the lavas were acquired in RTFA magma reservoirs through bulk assimilation and/or partial melting of crustal wall-rocks. Contamination was greatest for Nadezhdinsky-suite magmas, but processes in RTFA reservoirs also exerted a dominant control on the compositions of the chemically monotonous flood basalts that constitute the 2,300-m-thick third assemblage.
4) Earlier subdivision of Siberian flood-basalt volcanism into three assemblages (FEDORENKO, 1981) finds excellent support in our new geochemical and isotopic data and fits well within the context of the mantle-plume model.
5) Whereas certain suites of lavas in other CFB provinces pose difficulties for any model and point to additional controls during ascent through the continental lithospheric mantle, we suggest that processing of CFB magmas in RTFA magma reservoirs may be the norm rather than the exception.

Acknowledgments—We gratefully acknowledge Igor Migachev, Alexander Likhachev, and Alexey Volchkov of the Central Research Institute of Geological Prospecting for Base and Precious Metals for their strong support of our joint study. The Noril'sk State Nickel Concern and Noril'sk Expedition facilitated our collecting of samples in September 1990. The counsel of Joe Arth, Charlie Bacon, Tom Bullen, Wes Hildreth, Howard Wilshire, Mike Zientek, and other USGS colleagues throughout the course of this study is much appreciated. Richard Walker kept us informed of late-breaking developments on the Re-Os front. Joe Arth, Tom Bullen, Richard Carlson, Clark Johnson, John Mahoney, Stephen Moorbath, Bob Rapp, and George Tilton provided challenging reviews that contributed to our presentation. Susan Garcia provided excellent assistance with computer graphics. We greatly appreciate the editorial assistance of George Havach.

Editorial handling: G. Faure

REFERENCES

AL'MUKHAMEDOV A. I. and ZOLOTUKHIN V. V. (1988) Geochemistry of low-potassic basalts from Siberian and Deccan traps. In *Deccan Flood Basalts* (ed. K. V. SUBBARAO), pp. 341–351. Geological Society of India.

ARNDT N. T. and CHRISTENSEN U. (1992) The role of lithospheric mantle in continental flood volcanism: Thermal and geochemical constraints. *J. Geophys. Res.* **97**, 10,967–10,981.

ARNDT N. T., CZAMANSKE G. K., WOODEN J. L., and FEDORENKO

V. A. (1993) Mantle and crustal contributions to continental flood volcanism. *Tectonophysics.*

BACON C. R. and DRUITT T. H. (1988) Compositional evolution of the zoned calcalkaline magma chamber of Mount Mazama, Crater Lake, Oregon. *Contrib. Mineral. Petrol.* **98,** 224–256.

BAEDECKER P. A., ed. (1987) *Methods for Geochemical Analysis; USGS Bull. 1770.*

BRÜGMANN G. E., NALDRETT A. J., ASIF M., LIGHTFOOT P. C., GORBACHEV N. S., and FEDORENKO V. A. (1993) Siderophile and chalcophile metals as tracers of the evolution of the Siberian Trap in the Noril'sk region, Russia. *Geochim. Cosmochim. Acta* **57,** 2001–2018.

CAMPBELL I. H. and GRIFFITHS R. W. (1990) Implications of mantle plume structure for the evolution of flood basalts. *Earth Planet. Sci. Lett.* **99,** 79–93.

CAMPBELL I. H., CZAMANSKE G. K., FEDORENKO V. A., HILL R. I., STEPANOV V., and KUNILOV V. E. (1992) Synchronism of the Siberian traps and the Permian-Triassic boundary. *Science* **258,** 1760–1763.

CARLSON R. W. (1984) Isotopic constraints on Columbia River flood basalt genesis and the nature of the subcontinental mantle. *Geochim. Cosmochim. Acta* **48,** 2357–2372.

CARLSON R. W. (1991) Physical and chemical evidence on the cause and source characteristics of flood basalt volcanism. *Australian J. Earth Sci.* **38,** 525–544.

CARLSON R. W. and HART W. K. (1988) Flood basalt volcanism in the northwestern United States. In *Continental Flood Basalts* (ed. J. D. MACDOUGALL), pp. 35–62. Kluwer.

CLAOUÉ-LONG J. C., ZICHAO Z., GUOGAN M., and SHAOHUA D. (1991) The age of the Permian-Triassic boundary. *Earth Planet. Sci. Lett.* **105,** 182–190.

CONDIE K. K. (1993) Chemical composition and evolution of the upper continental crust: Contrasting results from surface samples and shales. *Chem. Geol.* (in press).

COX K. G. (1988) Numerical modelling of a randomized RTF magma chamber: A comparison with continental flood basalt sequences. *J. Petrol.* **29,** 681–699.

CZAMANSKE G. K., FEDORENKO V. A., LIND E. N., DALRYMPLE B. G., and WOODEN J. L. (1992a) The Siberian traps: A flip of the dynamo and 600,000 years of hell on earth? *Eos* **73,** 532 (abstr.).

CZAMANSKE G. K., KUNILOV V. E., ZIENTEK M. L., CABRI L. J., LIKHACHEV A. P., CALK L. C., and OSCARSON R. L. (1992b) A proton-microprobe study of sulfide ores from the Noril'sk-Talnakh district, Siberia. *Canadian Mineral.* **30,** 249–287.

DALRYMPLE G. B., CZAMANSKE G. K., LANPHERE M. A., STEPANOV V., and FEDORENKO V. (1991) $^{40}Ar/^{39}Ar$ ages of samples from the Noril'sk-Talnakh ore-bearing intrusions and the Siberian flood basalts. *Eos* **72,** 570 (abstr.).

DEPAOLO D. J. and WASSERBURG G. J. (1979) Nd isotopes in flood basalts from the Siberian Platform and inferences about their mantle sources. *Proc. Natl. Acad. Sci. USA* **76,** 3056–3060.

DODIN D. A. and GOLUBKOV V. S. (1971) A differentiated basalt sheet in the Noril'sk district in the northwestern part of the Siberian platform. *Dokl. Akad. Nauk SSSR* **198,** 56–59.

DUNCAN A. R., ERLANK A. J., and MARSH J. S. (1984) Regional geochemistry of the Karoo Igneous Province. *Geol. Soc. S. Africa Spec. Publ.* **13,** 355–388.

ELLAM R. M. and COX K. G. (1989) A Proterozoic lithospheric source for Karoo magmatism: Evidence from the Nuanetsi picrites. *Earth Planet. Sci. Lett.* **92,** 207–218.

ELLAM R. M. and COX K. G. (1991) An interpretation of Karoo picrite basalts in terms of interaction between asthenospheric magmas and the mantle lithosphere. *Earth Planet. Sci. Lett.* **105,** 330–342.

ELLAM R. M., CARLSON R. W., and SHIREY S. B. (1992) Evidence from Re-Os isotopes for plume-lithosphere mixing in Karoo flood basalt genesis. *Nature* **359,** 718–721.

FEDORENKO V. A. (1979) Paleotectonics of Late Paleozoic-Early Mesozoic volcanism in the Noril'sk region, and paleotectonic controls on the distribution of Ni-bearing intrusions. In *Geology and Ore Deposits of the Taymieria-Nortland Folding Belt* (ed. YU. YE. POGREBITSKY), pp. 16–23 (in Russian). NIIGA, Leningrad.

FEDORENKO V. A. (1981) Petrochemical series of extrusive rocks of the Noril'sk region. *Soviet Geol. Geophys.* **22**(6), 66–74.

FEDORENKO V. A. (1991) Tectonic control of magmatism and regularities of Ni-bearing localities on the northwestern Siberian platform. *Soviet Geol. Geophys.* **32**(1), 41–47.

FEDORENKO V. A. (1993) Evolution of magmatism as reflected in the volcanic sequence of the Noril'sk region. In *Proceedings of the Sudbury-Noril'sk Symposium* (ed. P. C. LIGHTFOOT et al.); *Ontario Geological Survey Special Volume 5.*

FEDORENKO V. A., STIFEEVA G. T., MAKEEVA L. V., SUKHAREVA M. S., and KUZNETSOVA N. P. (1984) Mafic and alkali-mafic intrusions of the Noril'sk region; their co-magmatic relation to the volcanic formations. *Soviet Geol. Geophys.* **25**(6), 54–61.

FURLONG K. P. and FOUNTAIN D. M. (1986) Continental crustal underplating: Thermal considerations and seismic-petrologic consequences. *J. Geophys. Res.* **91,** 8285–8294.

GRIFFITHS R. W. and CAMPBELL I. H. (1990) Stirring and structure in mantle starting plumes. *Earth Planet. Sci. Lett.* **99,** 66–78.

GRIFFITHS R. W. and CAMPBELL I. H. (1991) Interaction of mantle plume heads with the Earth's surface and onset of small-scale convection. *J. Geophys. Res.* **96,** 18,295–18,310.

HAAG M. and HELLER F. (1991) Late Permian to Early Triassic magnetostratigraphy. *Earth Planet. Sci. Lett.* **107,** 42–54.

HART S. R., HAURI E. H., OSCHMANN L. A., and WHITEHEAD J. A. (1992) Mantle plumes and entrainment: Isotopic evidence. *Science* **256,** 517–520.

HAWKESWORTH C. J., MARSH J. S., DUNCAN A. R., ERLANK A. J., and NORRY M. J. (1984a) The role of continental lithosphere in the generation of the Karoo volcanic rocks: Evidence from combined Nd- and Sr-isotope studies. *Geol. Soc. S. Africa Spec. Publ.* **13,** 341–354.

HAWKESWORTH C. J., ROGERS N. W., VAN CALSTEREN P. W. C., and MENZIES M. A. (1984b) Mantle enrichment processes. *Nature* **311,** 331–336.

HERGT J. M., CHAPPELL B. W., MCCULLOCH M. T., MCDOUGALL I., and CHIVAS A. R. (1989) Geochemical and isotopic constraints on the origin of the Jurassic dolerites of Tasmania. *J. Petrol.* **30,** 841–883.

HERGT J. M., PEATE D. W., and HAWKESWORTH C. J. (1991) The petrogenesis of Mesozoic Gondwana low-Ti flood basalts. *Earth Planet. Sci. Lett.* **105,** 134–148.

HERZBERG C., GASPARIK T., and SAWAMOTO H. (1990) Origin of mantle peridotite: Constraints from melting experiments to 16.5 GPa. *J. Geophys. Res.* **95,** 15,779–15,803.

HILDRETH W. and MOORBATH S. (1988) Crustal contributions to arc magmatism in the Andes of central Chile. *Contrib. Mineral. Petrol.* **98,** 455–489.

HOFMANN A. W. (1988) Chemical differentiation of the Earth: The relation between mantle, continental crust, and oceanic crust. *Earth Planet. Sci. Lett.* **90,** 297–314.

HOFMANN A. W., JOCHUM K. P., SEUFERT M., and WHITE W. M. (1986) Nb and Pb in oceanic basalts: New constraints on mantle evolution. *Earth Planet. Sci. Lett.* **79,** 33–45.

HUPPERT H. E. and SPARKS R. S. J. (1985) Komatiites I: Eruption and flow. *J. Petrol.* **26,** 694–725.

KUZNETSOV M. F. and NAUMOV V. A. (1975) Trap magmatism and some problems of tectonics in the southeast of the Tungusska syneclise. *Intl. Geol. Rev.* **17,** 781–785.

LIGHTFOOT P. C. and HAWKESWORTH C. J. (1988) Origin of Deccan Trap lavas: Evidence from combined trace element and Sr-, Nd- and Pb-isotope studies. *Earth Planet. Sci. Lett.* **91,** 89–104.

LIGHTFOOT P. C., HAWKESWORTH C. J., DEVEY C. W., ROGERS N. W., and VAN CALSTEREN P. W. C. (1990a) Source and differentiation of Deccan Trap lavas: Implications of geochemical and mineral chemical variations. *J. Petrol.* **31,** 1165–1200.

LIGHTFOOT P. C., NALDRETT A. J., GORBACHEV N. S., DOHERTY W., and FEDORENKO V. A. (1990b) Geochemistry of the Siberian trap of the Noril'sk area, USSR, with implications for the relative contributions of crust and mantle to flood basalt magmatism. *Contrib. Mineral. Petrol.* **104,** 631–644.

LIGHTFOOT P. C., HAWKESWORTH C. J., HERGT J., NALDRETT

A. J., GORBACHEV N. S., FEDORENKO V. A., and DOHERTY W. (1993a) Remobilization of the continental lithosphere by a mantle plume: Major-, trace-element, and Sr-, Nd- and Pb-isotopic evidence from picritic and tholeiitic lavas of the Noril'sk District, Siberia. *Contrib. Mineral. Petrol.* **114,** 171–188.

LIGHTFOOT P. C., HAWKESWORTH C. J., HERGT J., NALDRETT A. J., GORBACHEV N. S., FEDORENKO V. A., and DOHERTY W. (1993b) Chemostratigraphy of Siberian trap lavas, Noril'sk District, Russia: Implications for the evolution of flood basalt magmas. In *Proceedings of the Sudbury-Noril'sk Symposium* (ed. P. C. LIGHTFOOT et al.); *Ontario Geological Survey Special Volume 5.*

LIND E. N. and SCHEKOTUROV V. V. (1991) Paleomagnetic dating of the trap volcanism of the North-West of the Siberian platform. In *All Union Congress on Geomagnatism, Part II, Vladimir-Suzdal,* pp. 79–80 (in Russian). SNIO, USSR.

MAHONEY J. J. (1988) Deccan Traps. In *Continental Flood Basalts* (ed. J. D. MACDOUGALL), pp. 151–194. Kluwer.

MAKARENKO G. F. (1976) The epoch of Triassic trap magmatism in Siberia. *Intl. Geol. Rev.* **19,** 1089–1100.

MASLOV G. D. and NESTEROVSKY V. S. (1961) Explosive fragments of the crystalline basement in the Triassic tuffs. *Geol. Geophys.* **12,** 128–130 (in Russian).

MAURY R. C., DEFANT M. J., and JORON F.-L. (1992) Metasomatism of the sub-arc mantle inferred from trace elements in Philippine xenoliths. *Nature* **360,** 661–663.

MCDONOUGH W. F. (1990) Constraints on the composition of the continental lithospheric mantle. *Earth Planet. Sci. Lett.* **101,** 1–18.

MCDONOUGH W. F. (1992) Chemical and isotopic systematics of continental lithospheric mantle. *Proc. 5th Intl. Kimberlite Conf.,* 478–485.

MCKENZIE D. and BICKLE M. J. (1988) The volume and composition of melt generated by extension of the lithosphere. *J. Petrol.* **29,** 625–679.

MENZIES M. A. (1992) The lower lithosphere as a major source for continental flood basalts: A re-appraisal. In *Magmatism and the Causes of Continental Break-up* (ed. B. C. STOREY et al.); *Geol. Soc. Spec. Publ.* **68,** pp. 33–41.

MENZIES M. A., ROGERS N. W., TINDLE A., and HAWKESWORTH C. J. (1987) Metasomatic and enrichment processes in lithospheric peridotites, an effect of asthenosphere-lithosphere interaction. In *Mantle Metasomatism* (ed. M. A. MENZIES and C. J. HAWKESWORTH), pp. 313–361. Academic Press.

MILANOVSKIY YE. YE. (1976) Rift zones of the geologic past and their associated formations. Report 2. *Intl. Geol. Rev.* **18,** 619–639.

NALDRETT A. J., LIGHTFOOT P. C., FEDORENKO V., DOHERTY W., and GORBACHEV N. S. (1992) Geology and geochemistry of intrusions and flood basalts of the Noril'sk region, USSR, with implications for the origin of the Ni-Cu ores. *Econ. Geol.* **87,** 975–1004.

NICOLAS A. (1986) A melt extraction model based on structural studies in mantle peridotites. *J. Petrol.* **27,** 999–1022.

NICOLAS A. (1989) *Structures of Ophiolites and Dynamics of Oceanic Lithosphere.* Kluwer.

O'HARA M. J. (1977) Geochemical evolution during fractional crystallization of a periodically refilled magma chamber. *Nature* **266,** 503–507.

O'HARA M. J. (1980) Nonlinear nature of the unavoidable long-lived isotopic, trace and major element contamination of a developing magma chamber. *Phil. Trans. Roy. Soc. London* **A297,** 215–227.

O'HARA M. J. and MATHEWS R. E. (1981) Geochemical evolution in an advancing, periodically replenished, periodically tapped, continuously fractionated magma chamber. *J. Geol. Soc. London* **138,** 237–277.

PEARSON D. G., SHIREY S. B., CARLSON R. W., BOYD F. R., NIXON P. H., and POKHILENKO N. P. (1991) Re-Os and Sm-Nd isotopic constraints on the chronology of lithospheric mantle formation and enrichment events. *Eos* **72,** 527 (abstr.).

PEATE D. W., HAWKESWORTH C. J., and MANTOVANI M. S. M. (1992) Chemical stratigraphy of the Parana lavas (South America): Classification of magma types and their spatial distribution. *Bull. Volcanol.* **55,** 119–139.

PENG Z. X., MAHONEY J., HOOPER P., HARRIS C., and BEANE J. (1993) A possible role for lower continental crust in flood basalt genesis? Isotopic and incompatible element study of the lower six formations of the western Deccan traps. *Geochim. Cosmochim. Acta* (in press).

RAPP R. P. and WATSON E. B. (1993) Water-deficient partial melting of metabasalt at 8-32 kbar and continental growth. *J. Petrol.*

RAPP R. P., WATSON E. B., and MILLER C. F. (1991) Partial melting of amphibolite/eclogite and the origin of Archean trondjemites and tonalites. *Precambrian Res.* **51,** 1–25.

RICHARDS M. A., DUNCAN R. A., and COURTILLOT V. E. (1989) Flood basalts and hotspot tracks: Plume heads and tails. *Science* **246,** 103–107.

RUDNICK R. L. (1992) Xenoliths—Samples of the lower continental crust. In *The Continental Lower Crust* (ed. D. M. FOUNTAIN et al.), pp. 269–316. Elsevier.

RUDNICK R. L. and PRESPER T. (1990) Geochemistry of intermediate to high-pressure granulites. In *Granulites and Crustal Evolution* (ed. D. VIELZEUF and P. VIDAL), pp. 523–568. Kluwer.

RUDNICK R. L., MCDONOUGH W. F., MCCULLOCH M. T., and TAYLOR S. R. (1986) Lower crustal xenoliths from Queensland, Australia: Evidence for deep crustal assimilation and fractionation of continental basalts. *Geochim. Cosmochim. Acta* **50,** 1099–1115.

RYABOV V. V., BAKUMENKO I. T., and FOMUNYKH I. M. (1977) Dendritic megacrysts of clinopyroxene in traps of the Noril'sk district and some questions about their formation. *Akad. Nauk SSSR, Sibirskoe Otdelenie, Inst. Geol. Geof. Trudy* **349,** 47–74 (in Russian).

RYABOV V. V., KONENKO V. F., and KHMEL'NIKOVA O. S. (1985) Rock-forming minerals of picritic basalts of the Noril'sk region. *Soviet Geol. Geophys.* **26**(4), 77–84.

SHARMA M., BASU A. R., and NESTERENKO G. V. (1991) Nd-Sr isotopes, petrochemistry, and origin of the Siberian flood basalts, Siberia. *Geochim. Cosmochim. Acta* **55,** 1183–1192.

SHARMA M., BASU A. R., and NESTERENKO G. V. (1992) Temporal Sr-, Nd-, and Pb-isotopic variations in the Siberian flood basalts: Implications for the plume-source characteristics. *Earth Planet. Sci. Lett.* **113,** 365–381.

SPENCE D. A. and TURCOTTE D. L. (1990) Buoyancy-driven magma fracture: A mechanism for ascent through the lithosphere and the emplacement of diamonds. *J. Geophys. Res.* **95,** 5133–5139.

STACEY J. S. and KRAMERS J. D. (1975) Approximation of terrestrial lead isotopic evolution by a two stage model. *Earth Planet. Sci. Lett.* **26,** 207–221.

SUN S.-S. and MCDONOUGH W. F. (1989) Chemical and isotopic systematics of oceanic basalts: Implications of mantle composition and processes. In *Magmatism in the Ocean Basins* (ed. A. D. SAUNDERS and M. J. NORRY); *Geol. Soc. Spec. Publ.* **42,** pp. 313–345.

TAKAHASHI E. (1986) Melting of a dry peridotite KLB1 up to 14 GPa: Implications on the origin of peridotite upper mantle. *J. Geophys. Res.* **91,** 9367–9382.

TAKAHASHI E. (1992) Evolution of the Earth's mantle: Implications of high pressure experimental studies on basalts and peridotites. *Evolving Earth Symposium,* Okazaki 1992, p. 167 (abstr.).

TAYLOR S. R. and MCLENNAN S. M. (1985) *The Continental Crust: Its Composition and Evolution.* Blackwell.

VOSHAGE H., HOFMANN A. W., MAZZUCCHELLI M., RIVALENTI G., SINIGOI S., RACZEK I., and DEMARCHI G. (1990) Isotopic evidence from the Ivrea zone for a hybrid lower crust formed by magmatic underplating. *Nature* **347,** 731–736.

WALKER R. J., MORGAN J. W., CZAMANSKE G. K., LIKHACHEV A. P., and KUNILOV V. E. (1992) Re-Os isotopic evidence for a plume origin for Noril'sk-Talnakh ores and associated ultramafic rocks: Siberia, Russia. *Eos* **73,** 626 (abstr.).

WALKER R. J., MORGAN J. W., HORAN M. F., CZAMANSKE G. K., KROGSTAD E. J., LIKHACHEV A. P., and KUNILOV V. E. (1993) Re-Os isotopic evidence for an enriched mantle-plume source for the Noril'sk-type ore-bearing intrusions, Siberia. *Geochim. Cosmochim. Acta* (in press).

WHEATLEY M. R. and ROCK N. M. S. (1988) SPIDER: A Macintosh program to generate normalized multi-element "spidergrams." *Amer. Mineral.* **73**, 919–921.

WHITE W. M. and PATCHETT P. J. (1984) Hf-Nd-Sr isotopes and incompatible element abundances in island arcs: Implications for magma origins and crust-mantle evolution. *Earth Planet. Sci. Lett.* **67**, 167–185.

WINTHER K. T. and NEWTON R. C. (1990) Experimental melting of hydrous low-K tholeiite: Evidence on the origin of Archaean cratons. *Bull. Geol. Soc. Denmark* **39**, 213–228.

WOODEN J. L., CZAMANSKE G. K., BOUSE R. M., KNIGHT R. J., and BUDAHN J. R. (1992) Pb isotopic data indicate a complex, mantle origin for the Noril'sk-Talnakh ores, Siberia. *Econ. Geol.* **87**, 1153–1165.

ZEN'KO T. E. and CZAMANSKE G. K. (1993) Physical and petrologic aspects of the intrusions of the Noril'sk-Talnakh area, Siberia. In *Proceedings of the Sudbury-Noril'sk Symposium* (ed. P. C. LIGHTFOOT et al.); *Ontario Geological Survey Special Volume 5.*

ZOLOTUKHIN V. V. and AL'MUKHAMEDOV A. I. (1988) Traps of the Siberian Platform. In *Continental Flood Basalts* (ed. J. D. MACDOUGALL), pp. 273–310. Kluwer.

ZOLOTUKHIN V. V. and AL'MUKHAMEDOV A. I. (1990) Fractionation and alkalinity in the evolution of the source magmas of platform basites (by example of the northwestern Siberian platform). *Soviet Geol. Geophys.* **31**(10), 15–21.

ZOLOTUKHIN V. V. and AL'MUKHAMEDOV A. I. (1991) Problems of trap magmatism of platforms. *Soviet Geol. Geophys.* **32**(1), 26–34.

ZONENSHAIN L. P., KUZMIN M. I., and NATAPOV L. M. (1990) *Geology of the USSR: A Plate-Tectonic Synthesis. Geodynamics Series*, Vol. 21. American Geophysical Union, Washington, DC.

ZORIN Y. A. and VLADIMIROV B. M. (1989) On the genesis of trap magmatism of the Siberian platform. *Earth Planet. Sci. Lett.* **93**, 109–112.